Microbiological Research 247 (2021) 126730

Contents lists available at ScienceDirect

Microbiological Research

journal homepage: www.elsevier.com/locate/micres

iTRAQ-based proteomic analysis of *Paracoccidioides brasiliensis* in response to hypoxia

Lucas Nojosa Oliveira [a], Patrícia de Sousa Lima [a], Danielle Silva Araújo [a], Igor Godinho Portis [a], Agenor de Castro Moreira dos Santos Júnior [b], Alexandre Siqueira Guedes Coelho [c], Marcelo Valle de Sousa [b], Carlos André Ornelas Ricart [b], Wagner Fontes [b], Célia Maria de Almeida Soares [a,*]

[a] Laboratório de Biologia Molecular, Instituto de Ciências Biológicas, ICB II, Campus II, Universidade Federal de Goiás, 74001-970, Goiânia, Goiás, Brazil
[b] Departmento de Biologia Celular, Instituto de Biologia, Universidade de Brasília, Campus Darcy Ribeiro, Asa Norte, 70910-900, Brasília, DF, Brazil
[c] Laboratório de Genética e Genômica de Plantas, Escola de Agronomia, Universidade Federal de Goiás, Goiânia, Brazil

ARTICLE INFO

Keywords:
Low oxygen
*Pb*18
Isobaric tag proteomics

ABSTRACT

Aerobic organisms require oxygen for energy. In the course of the infection, adaptation to hypoxia is crucial for survival of human pathogenic fungi. Members of the *Paracoccidioides* complex face decreased oxygen tensions during the life cycle stages. In *Paracoccidioides brasiliensis* proteomic responses to hypoxia have not been investigated and the regulation of the adaptive process is still unknown, and this approach allowed the identification of 216 differentially expressed proteins in hypoxia using iTRAQ-labelling. Data suggest that *P. brasiliensis* reprograms its metabolism when submitted to hypoxia. The fungus reduces its basal metabolism and general transport proteins. Energy and general metabolism were more representative and up regulated. Glucose is apparently directed towards glycolysis or the production of cell wall polymers. Plasma membrane/cell wall are modulated by increasing ergosterol and glucan, respectively. In addition, molecules such as ethanol and acetate are produced by this fungus indicating that alternative carbon sources probably are activated to obtain energy. Also, detoxification mechanisms are activated. The results were compared with label free proteomics data from *Paracoccidioides lutzii*. Biochemical pathways involved with acetyl-CoA, pyruvate and ergosterol synthesis were up-regulated in both fungi. On the other hand, proteins from TCA, transcription, protein fate/degradation, cellular transport, signal transduction and cell defense/virulence processes presented different profiles between species. Particularly, proteins related to methylcitrate cycle and those involved with acetate and ethanol synthesis were increased in *P. brasiliensis* proteome, whereas GABA shunt were accumulated only in *P. lutzii*. The results emphasize metabolic adaptation processes for distinct *Paracoccidioides* species.

1. Introduction

Currently, thousands of people are infected with *Paracoccidioides* spp.; they are thermally dimorphic fungi responsible for the neglected systemic mycosis, paracoccidioidomycosis (PCM) (Martinez, 2017; Queiroz-Telles et al., 2017; Rodrigues and Nosanchuk, 2020; Teixeira et al., 2014). This disease is endemic in Latin America, and around 80 % of infected patients live in Brazil (Martinez, 2017), representing approximately 49 % of hospital admissions among all mycoses (Coutinho et al., 2015). The disease accounts for 51 % of deaths due to systemic mycoses in immunocompetent individuals (Prado et al., 2009).

For the establishment of infection several molecular mechanisms are engineered by members of the *Paracoccidioides* genus in an attempt to evade the potent defense arsenal of the host's immune system (Mendes-Giannini et al., 2005). *Paracoccidioides* yeast cells can survive the stresses imposed by the host (Mendes et al., 2017) developing a chronic disease in the majority (74–96 %) of patients (Shikanai-Yasuda et al., 2017). The genus comprises five species: *Paracoccidioides brasiliensis*,

* Corresponding author at: Laboratório de Biologia Molecular, Instituto de Ciências Biológicas II, Câmpus Samambaia, Universidade Federal de Goiás, 74690-900, Goiânia, Goiás, Brazil.

E-mail addresses: nojosalucas@gmail.com (L.N. Oliveira), pathricialima@gmail.com (P.S. Lima), daniellebiomedaraujo@gmail.com (D.S. Araújo), igorportis@gmail.com (I.G. Portis), agenor.unb@gmail.com (A.C.M. Santos Júnior), alexandre.coelho@icloud.com (A.S.G. Coelho), mvsousa@unb.br (M.V. de Sousa), ricart@unb.br (C.A.O. Ricart), wagnerfontes2@gmail.com (W. Fontes), cmasoares@gmail.com (C.M.A. Soares).

https://doi.org/10.1016/j.micres.2021.126730
Received 5 June 2020; Received in revised form 29 January 2021; Accepted 13 February 2021
Available online 18 February 2021

Paracoccidioides lutzii, *Paracoccidioides americana*, *Paracoccidioides restrepiensis* and *Paracoccidioides venezuelensis* (Turissini et al., 2017) without described correlation with clinical forms of the disease (Shikanai-Yasuda et al., 2017).

In mammalian tissues oxygen levels are considered low comparing with the atmosphere (Erecińska and Silver, 2001; He et al., 1999; Karhausen et al., 2004). In the course of infection, pathogenic fungi face reduced oxygen (hypoxia) environment and numerous metabolic adaptations can guarantee their survival (Grahl et al., 2012; He et al., 1999). In fungi, few aspects of sensing, signaling, and transcriptional regulatory mechanisms of hypoxia adaptation have been characterized (Butler, 2013; Hillmann et al., 2015, 2014; Oliveira et al., 2020). Hypoxia has been considered a relevant condition to virulence of fungi such as *Cryptococcus neoformans* and *Aspergillus fumigatus* (Chun et al., 2007; Willger et al., 2008). In general, fungi submitted to hypoxic environment regulate the expression of genes associated with respiration, heme, lipid and membrane biosynthesis, cell wall structure, and other metabolic pathways (González Siso et al., 2012; Hillmann et al., 2015). However, such responses and their regulatory mechanisms are varied in different fungal species and several models of low oxygen sensing have been proposed (Butler, 2013; Hillmann et al., 2015). The main fungi hypoxic sensor is the homologue of mammalian SREBP (sterol regulatory element binding protein) (Espenshade, 2006; Espenshade and Hughes, 2007) first identified and characterized in the fission yeast *Schizosaccharomyces pombe* (Hughes et al., 2005; Todd et al., 2006). Later, other fungi had this homologue characterized: *C. neoformans*, *A. fumigatus*, *Histoplasma capsulatum* and *P. lutzii* (Chang et al., 2007; Chun et al., 2007; Dubois et al., 2016; Lima et al., 2015; Willger et al., 2008). SREBP homologues control the expression of genes involved in biosynthesis of lipids, ergosterol, and heme (Chang et al., 2007; Chun et al., 2007; Willger et al., 2008).

In order to clarify how adaptation to hypoxia occurs, transcriptomic and proteomic data in response to oxygen limitation have been obtained in several species of fungi; overall, the results show a radical change in energy obtaining, besides relevant changes in morphology, virulence and susceptibility to drugs, determinant aspects for their survival (Chang et al., 2007; Chun et al., 2007; de Groot et al., 2007; Dubois et al., 2016; Grahl et al., 2012; Lima et al., 2015; Shimizu et al., 2009; Vödisch et al., 2011). In *P. lutzii*, *Pl*01, responses to hypoxic stress, were changes in metabolic pathways such as glycolysis, TCA, beta-oxidation, mitochondrial electron transport and GABA shunt (Lima et al., 2015).

Proteomic approaches have revealed important metabolic differences in the *Paracoccidioides* genus. A closer look at the dimorphic process showed that during the mycelial phase, glycolysis and alcoholic fermentation are predominant in *P. brasiliensis* (Araújo et al., 2019) while in *P. lutzii* this profile is found in the yeast phase (Rezende et al., 2011; Tavares et al., 2015). During growth in glucose as carbon source, the energy metabolism among *Paracoccidioides* species was distinct. Yeast cells of *Pb*EPM83, member of the *P. restrepiensis* species, preferentially uses aerobic routes for energy production using the glycolytic and TCA pathways. *Pb*2, *P. americana* species, prioritizes the pentose phosphate pathway and amino acid degradation and *Pb*339, belonging to the *P. brasiliensis* species, preferentially performs beta oxidation, in contrast to *Pl*01 which is a member of the *P. lutzii* species, that preferably uses anaerobic metabolism, alcoholic fermentation (Pigosso et al., 2013). In acetate, as the only carbon source, gluconeogenesis and amino acid degradation presented the same profile among species, but beta oxidation and methylcitrate cycle were increased in *Pl*01 and *Pb*EPM83 (Baeza et al., 2017).

In this study, the proteome of *P. brasiliensis* submitted to hypoxia was obtained and data suggest that this fungus reduces its basal metabolism as demonstrated by decreased levels of proteins related to cell cycle, DNA maintenance and transcription. General and organelle specific transport proteins were down-regulated as well. Glucose is apparently directed towards glycolysis or the production of cell wall polymers, such as glucan to compensate the hypoxia negative effect in this structure. Ergosterol increased in *P. brasiliensis* submitted to hypoxia. Moreover, peroxisomal beta-oxidation was activated producing hydrogen peroxide, acetyl-CoA, and propionyl-CoA. Acetyl-CoA is important to ergosterol accumulation while propionyl-CoA feeds the methylcitrate cycle, which produces pyruvate that, in turn, produces ethanol and acetate, possible alternative carbon sources used by *P. brasiliensis* in this context.

The proteomes of *P. brasiliensis* (*Pb*18) and *P. lutzii* (*Pl*01) (Lima et al., 2015) during hypoxia were compared. Both species increased the expression of proteins related to acetyl-CoA, pyruvate and ergosterol synthesis and reduces those involved with the pentose phosphate pathway. The opposite profile was related with TCA cycle, which was up-regulated in *P. brasiliensis* and down-regulated in *P. lutzii*. On the other hand, proteins belonging to transcription, protein fate/-degradation, cellular transport, signal transduction and cell defense/-virulence processes were decreased in *P. brasiliensis* and increased in *P. lutzii*. Some biological categories were increased only in *P. brasiliensis* such as methylcitrate cycle and those involved with acetate and ethanol synthesis, whereas the GABA shunt was increased only in *P. lutzii*.

iTRAQ-based proteomic analysis is an elegant and robust technique and has been widely used in several quantitative proteomics studies. This work details the protein profile during oxygen deprivation, highlighting proteins that were differentially expressed. Hypoxia is experienced by the fungus during infection. The focus on fungus metabolic and structural remodeling can increase the understanding of the parasite-host relationship. Furthermore, this work serves as a basis for choosing proteins to be studied as therapeutic targets soon.

2. Material and methods

2.1. Growth conditions

P. brasiliensis (*Pb*18, ATCC 32069) was used in all experiments, in biological triplicates. The yeast cells were maintained for 5 days, at 36 °C in BHI solid medium supplemented with 4 % (w/v) glucose. To obtain exponential growth, cells were collected and seeded in BHI liquid medium also supplemented with 4 % (w/v) glucose at 36 °C for 72 h. Then, cells were centrifuged and washed using PBS 1X (phosphate buffer solution). The same amount of *Pb*18 viable cells (a total of 10^6) were seeded in a new BHI medium plus 4 % (w/v) glucose at 36 °C under normoxia and hypoxia for 12 h. Normoxic conditions were considered atmospheric levels inside the lab (~21 % O_2). For hypoxic-mimetic conditions, a controlled chamber multi-gas (Multi-Gas Incubator MCO-19M-UV, Panasonic Biomedical) was kept at gas mixture containing 1 % O_2, 5 % CO_2 and 94 % N_2 (Lima et al., 2015).

2.2. Protein extraction

Yeast cells cultivated in normoxia and hypoxia were harvested at time-point of 12 h. For each experimental condition, biological triplicates were obtained. Protein extraction was performed as previously described (Villén and Gygi, 2008). Briefly, the cells were re-suspended in cold extraction buffer (8 M urea, 75 mM NaCl, 50 mM Tris, pH 8.2, 50 mM β-glycerophosphate, 1 mM sodium orthovanadate, 10 mM sodium pyrophosphate and 1 mM PMSF). After, the cells were disrupted by vigorous mixing with glass beads, processed on ice in a beadbeater apparatus for four cycles of 90 s, in maximum speed. Then, lysates were centrifuged at 15,000 x *g* for 15 min at 4 °C until no pellet formation was obtained, and the supernatant was recovered. Proteins concentrations were estimated using a Qubit™ protein assay kit (Invitrogen) according to the manufacturer's procedures.

2.3. In-solution protein digestion

Estimated 150 μg of the protein extract of each condition/replicate was prepared for trypsin digestion as described (Queiroz et al., 2014)

with slight modifications. Cold acetone was added to the protein suspension and the mixture was vortexed and incubated overnight at −20 °C. After, the samples were centrifuged at 20,000 x *g* for 15 min at 4 °C and re-suspended in 8 M urea in 0.05 M triethylammonium bicarbonate – TEAB, pH 7.9. Next, proteins were reduced with 0.005 M DTT for 25 min at 55 °C and alkylated with 0.014 M iodoacetamide for 40 min at room temperature in dark. Samples were diluted 5-fold with 0.001 M $CaCl_2$ in 0.025 M TEAB, pH 7.9. Modified trypsin (Promega, Madison, WI, USA) was added in 1:50 (w/w) substrate ratio and samples were incubated overnight at 37 °C. The peptide samples were acidified with 0.1 % (v/v) TFA and desalted on homemade C18 microcolumns in P200 low-binding tips. Thereafter, all samples were dried in speed vacuum.

2.4. Isobaric tag labelling

The peptide mixtures from the biological triplicates were labeled with iTRAQ (Sciex) according to manufacturer's procedures. Fifty micrograms of the desalted and dried peptides were resuspended in 17 µL of 300 mM TEAB. The iTRAQ tag was resuspended in 70 µL of ethanol, and added. The samples were incubated for 2 h at room temperature. Equimolar amounts of iTRAQ label were mixed in all samples (normoxia labeled with 114; hypoxia with 117, see Supplementary Fig. 1).

2.5. LC–MS/MS

iTRAQ labelled peptides were analyzed with three biological repetitions each and separated using a nano-UHPLC Dionex Ultimate 3000 (Thermo Fisher Scientific) coupled with an Orbitrap Elite™ Hybrid Ion Trap-Orbitrap Mass Spectrometer (Thermo Fisher Scientific). Each fraction was loaded onto a pre-column (110 µm x200 nm) packed in-house with C18 ResiproSilPur of 5 µm with 120 Å pores (Dr. Maisch GmbH, Ammerbuch, Germany). Second chromatography was carried out in column (75 µm x35 nm) packed in-house with C18 ResiproSilPur of 3 µm with 120 Å pores (Dr. Maisch GmbH, Ammerbuch, Germany) and eluted using a gradient from 100 % solvent A [0.1 % (v/v) formic acid] to 26 % solvent B [0.1 % (v/v) formic acid, 95 % (v/v) acetonitrile] for 180 min, followed from 26 % to 100 % solvent B for 5 min and 100 % solvent B for 8 min (a total of 193 min at 200 nL/min). After each run, the column was washed with 90 % solvent B and re-equilibrated with solvent A. Mass spectra were acquired in positive ion mode applying data-dependent automatic survey MS scan and tandem mass spectra (MS/MS) acquisition modes. Each MS scan in the Orbitrap analyzer (mass range = m/z 350–1800, resolution = 120,000) was followed by MS/MS of the fifteen most intense ions in the LTQ. Fragmentation in the LTQ was performed by high-energy collision-induced dissociation (HCD), and selected sequenced ions sequences were dynamically excluded every 15 s.

2.6. MS spectra process

Raw data processing was performed using Proteome Discoverer v.1.3 beta (Thermo Scientific). The Raw files were submitted to a database search using Proteome Discoverer with Mascot v.2.3 algorithm against the *P. brasiliensis* database, downloaded using the Database on Demand tool in UniProt/SWISS-PROT (http://www.uniprot.org/) and NCBI (www.ncbi.nlm.nih.gov/genome/?term=Paracoccidioides) database. The searches were performed with the following parameters: MS accuracy - 10 ppm; MS/MS accuracy - 0.05 Da; two missed cleavage sites allowed; carbamidomethylation of cysteine as a fixed modification; and oxidation of methionine, N-terminal iTRAQ tagging and protein N-terminal acetylation as variable modifications. The numbers of proteins, protein groups, and peptides were filtered for false discovery rates less than 1 %. A minimum of two peptides per protein was accepted for identification using Proteome Discoverer. The identification lists from technical repetitions were merged, and repeated protein groups were removed. The mass spectrometry proteomics data have been deposited to the ProteomeXchange Consortium (http://www.proteomexchange.org/) via the PRIDE (Perez-Riverol et al., 2019) partner repository with the dataset identifier PXD019029.

2.7. Data analysis

The data consisted of three replicates containing global proteome. To increase the reliability, the acceptance criteria were applied, as following: proteins identified with at least two peptides (at least one unique peptide), with high or medium FDR and in at least 2 of 3 replicates (Araújo et al., 2019; Petito et al., 2020). The quantification values of each iTRAQ-labeled peptide were verified for labeling efficiency and equal mixing of channels, showing a very similar distribution across channels and replicates (Supplementary Fig. 1). The quantification values of each iTRAQ-labeled were log-transformed and applied unpaired Student's *t*-test. Statistical difference was set at p-value ≤ 0.05 and significant difference was set at p-value ≤ 0.01 (Yao et al., 2018). To determine up and down regulated proteins hypoxia/normoxia ratio was determined. Functional categories were determined by search in Blast2GO platform (http://www.blast2go.com/b2ghome), UniProt (https://www.uniprot.org/), Pedant on MIPS-Functional Catalogue (http://pedant.helmholtz-muenchen.de/) and KEGG database (http://www.genome.jp/kegg/). Sequence annotation was assessed using a BlastP algorithm (http://blast.ncbi.nlm.-nih.gov/Blast.cgi). All on-line algorithms were used in default parameters.

2.8. Cells labelling

P. brasiliensis yeast cells cultivated in biological triplicate under normoxia and hypoxia were collected at density of 10^6 cells and incubated with 400 µM of MitoTracker Green FM (Sigma-Aldrich), or 1.2 µM of Rhodamine 123 (Sigma-Aldrich) for 30 min at 36 °C in order to evaluate mitochondrial integrity and functionality, respectively. Glucan levels were measured by dying with 100 % (v/v) of Aniline Blue (AB, Sigma-Aldrich) for 5 min at room temperature under stirring. Levels of chitin were assessed after dying with 100 µg/mL of Calcofluor White (CFW, Sigma-Aldrich) for 15 min at room temperature. After dye incubation, the samples were washed twice with PBS 1X and the stained suspension was observed using Axio-Scope A1 Microscope (Carl Zeiss AG, Germany). The minimum of 50 cells for each microscope slides, in triplicates for each replicate, were assessed to measure the fluorescence intensity (in pixels) through the AxioVision Software (Carl Zeiss AG, Germany). Statistical comparisons were performed using the Student's *t*-test and p-values ≤ 0.05 were considered statistically significant.

2.9. Enzymatic activities

All enzymatic assays were performed in biological triplicate. To determine Cytochrome C Oxidase (CCO) activity, we used the Cytochrome C Oxidase Assay Kit (Sigma Aldrich – CYTOCOX1) as determined by the manufacturer. The CCO activity was evaluated by a colorimetric assay based on observation of the decrease in absorbance of Ferrocytochrome C at 550 nm caused by its oxidation to Ferricytichrome C by CCO. Methylcitrate synthase activity was determined as described previously (Brock et al., 2000; Santos et al., 2020). Briefly, the reaction mixtures (1 mL) contained 50 mM Tris-HCl (pH 8.0), 1 mM 5, 5′-Dithiobis(2-nitrobenzoic acid) (DTNB, Sigma Aldrich), 1 mM oxaloacetate, 0.2 mM propionyl-CoA and the assays were started by adding the protein extracts (3 µg). The reaction was followed spectrophotometrically by measuring changes in A_{412} at 25 °C. One unit of enzyme activity was defined as the amount of enzyme producing 1 µmol min^{-1} of CoASH under the assay conditions. Formamidase activity was determined as described (Borges et al., 2010). The amount of ammonia released by each sample was determined by comparing to a standard curve. One unit (U) of formamidase specific activity was defined as the amount of enzyme required to hydrolyze 1 mmol of formamide

(corresponding to the formation of 1 mmol of ammonia) per min per mg of total protein. The results were considered statistically significant at p-values ≤ 0.01 by Student's *t*-test.

2.10. Biochemical tests

Intracellular ethanol concentration was measured by the Ethanol UV-method, R-Biopharm enzymatic detection kit as described in manufacturer's instructions (Darmstadt, Germany). This assay measures the amount of NADH released after the oxidation of ethanol to acetaldehyde followed by oxidation of acetaldehyde to acetic acid. The total of 10^8 *P. brasiliensis* yeast cells was recovered after normoxic and hypoxic incubation for 12 h, in biological triplicates. Free thiol levels were determined using DTNB reagent (Sigma Aldrich). A total of 10^6 *P. brasiliensis* yeast cells were obtained after normoxic and hypoxic incubation, in biological triplicate, and lysed as described by (Pigosso et al., 2017). After centrifugation, 100 mL of the supernatant was added to 100 mL of 500 mM phosphate buffer, pH 7.5, followed by the addition of 20 mL of 1 mM DTNB. Absorbance was measured at 412 nm using a plate reader. Total intracellular sterols dosage was performed to determine the amount of ergosterol in yeast cells, as previously reported with slight modifications (Arthington-Skaggs et al., 1999; Neto et al., 2014; Portis et al., 2020). Five grams of *P. brasiliensis* yeast cells were obtained after normoxia and hypoxia and collected by centrifugation. The wet weight of the cell pellet was determined for each biological triplicate and condition. Cells were washed three times using sterile PBS 1X . A total of 5 mL of 25 % alcoholic potassium hydroxide solution (25 g of KOH and 35 mL of sterile distilled water, brought to 100 mL with 100 % ethanol), was added to each pellet and vortex mixed for 2 min. The cell suspensions were incubated in an 85 °C water bath for 3 h and allowed to cool to room temperature. Sterols were extracted by addition of 2 mL of sterile distilled water and 5 mL *n*-heptane (Sigma-Aldrich), followed by vigorous mixing in a vortex mixer for 5 min. The samples were kept at room temperature for 1–2 h to allow the phases to separate or were stored at 4 °C overnight. One mL of the heptane layer (containing ergosterol) was transferred to a 1.5 mL tube and stored at −20 °C for as long as 24 h. Prior to analysis, a 150 μL aliquot of sterol extract was diluted 5-fold in 100 % ethanol and scanned spectrophotometrically in the range of 240 and 300 nm using a SpectraMax® Paradigm® Multi-Mode Detection Platform (Molecular Devices, San Jose, CA). The ergosterol content as a percentage of the wet cell weight was calculated by the following equations: value 1 = $[(A_{281.5}/290) \times F]$/wet cell weight, value 2 = $[(A_{230}/518) \times F]$/wet cell weight, and percent ergosterol = value 1 - value 2. "F" is the dilution factor in ethanol, and 290 and 518 are fixed values determined for crystalline ergosterol and dihydroergosterol, respectively. The glucose consumption by the cells was determined using an enzymatic system based in glucose oxidase and peroxidase reactions (Doles®) from culture supernatant. *P. brasiliensis* yeast cells cultivated in biological triplicate under normoxia and hypoxia and supernatant were collected. Brief, the glucose oxidase catalyzes the oxidation of glucose forming a red antipyrilquinonimine whose color intensity is proportional to the glucose concentration in the sample (510 nm). Absorbance measure was performed using the SpectraMax® Paradigm® Multi-Mode Detection Platform (Molecular Devices, San Jose, CA).

3. Results and discussion

3.1. The proteome of P. brasiliensis yeast cells in hypoxia

Paracoccidioides spp. can adapt to several adverse conditions in host as demonstrated *in vitro*. Those conditions include oxidative (Chaves et al., 2017; Grossklaus et al., 2013), nitrosative (Parente et al., 2015), and osmotic stresses (Rodrigues et al., 2016). Also deprivation of nutrients, such as glucose (Lima et al., 2014), oxygen (Lima et al., 2015), metals (de Curcio et al., 2017; Parente et al., 2013, 2011; Petito et al., 2020) or excess of metal (Portis et al., 2020) were investigated. *In vivo* and *ex vivo* conditions were also analyzed (Chaves et al., 2019; Parente-Rocha et al., 2015; Pigosso et al., 2017). During infection, the fungus finds several of the stresses cited above. It is known that, after intranasal inhalation, in the first hours, *Paracoccidioides* cells are able of establishing lung infection (Pigosso et al., 2017) and pulmonary oxygen concentrations can influence this process. Thus, we decided to mimic the hypoxia conditions to analyze proteome during this condition/time. This study model allows the refinement of data for the choice of target molecules for future studies.

For this, total extracts of *Pb*18 yeast cells submitted to normoxia (atmospheric oxygen tensions) and hypoxia (1 % O_2) at the 12 h' time-set were obtained. First, protein extracts were evaluated on SDS-PAGE. The result shows the high quality of the protein extraction (Supplementary Fig. 2A). Then, in-solution trypsin digestion followed by iTRAQ-labeling peptides were performed and samples were analyzed by liquid chromatography in tandem mass spectrometry (LC–MS/MS). In order to verify the quality of digestion, a preliminary analysis was carried out showing evidence of good protein identification (Supplementary Fig. 2B, left). MS spectra results after iTRAQ- labelling revealed the identification of 5,997 identified peptides, resulting in 1,190 protein hits containing 5,643 unique peptides (Supplementary Fig. 2B, right; Supplementary Tables 1 and 2; PRIDE dataset identifier PXD019029). Raw data of proteins and peptides obtained from the MS Amanda 2.0 from Proteome Discoverer v.1.3 beta (Thermo Scientific) are available in Supplementary Tables 1 and 2, respectively. The dynamic range chart depicted measured abundance of 4.5–5 $\log_{10}$ orders of magnitude, indicating a satisfactory detection distribution of a high and low proteins concentrations levels (Supplementary Figs. 2C and 1D). In addition, 68 and 67 % of the total identified proteins have ≥ 2 peptides per protein (Supplementary Fig. 2E) and ≥ 2 unique peptides identified per protein (Supplementary Fig. 2F). Altogether, these results show that all proteomic data are of good quality.

One thousand one hundred and ninety proteins were identified by iTRAQ-LC–MS/MS method and proteins with high FDR confidence and found in at least two replicates were selected for further analysis (Supplementary Fig. 2G). Next, the Student's *t*-test at p-value ≤ 0.01 was used as a threshold to determine the differentially accumulated proteins, as described in Yao and co-workers (Yao et al., 2018). Hypoxia/normoxia ratio was used to determine up regulated (>1) and down regulated (<1) proteins; supplementary tables 3 and 4 summarize all differentially expressed proteins. As result, *Pb*18 presented 76 and 140 significantly increased and decreased proteins, respectively, in hypoxia compared to normoxia (control).

Several biological processes were modulated in *Pb*18 cells at 12 h of hypoxia (Tables S3 and S4, Supplementary Fig. 3). Proteins related to metabolism and energy classifications were more representative as up than down regulated (Supplementary Fig. 3A). Other categories such as cell cycle and DNA maintenance, protein fate, transcription, protein fate/degradation and transport showed a higher number of proteins with reduced than increased expression (Supplementary Fig. 3B) indicating that core cellular processes are decreased by hypoxia in *Pb*18. Interesting, proteins related to cell rescue, defense and virulence demonstrated the same tendency in hypoxia comparing to normoxia.

3.1.1. Hypoxia promotes increased glycolysis and cell wall remodeling

Hypoxia stimulates remodeling of the energy metabolism in *Pb*18 as depicted in Fig. 1. Regarding carbohydrate metabolism, data showed that glycolysis is activated. The enzymes enolase (PADG_04059 accession number) and phosphoglycerate kinase (PADG_01896) were up-regulated (Table S2; Fig. 1). However, phosphoenolpyruvate carboxykinase (PEPKC - PADG_08503) was also increased in our data (Table S2; Fig. 1). This enzyme is classically related to gluconeogenesis in *Escherichia coli* catalyzing the decarboxylation and mononucleotide-dependent phosphorylation of oxaloacetate (OXA) to form phosphoenolpyruvate (PEP) (Goldie and Sanwal, 1980; Matte et al., 1997). This

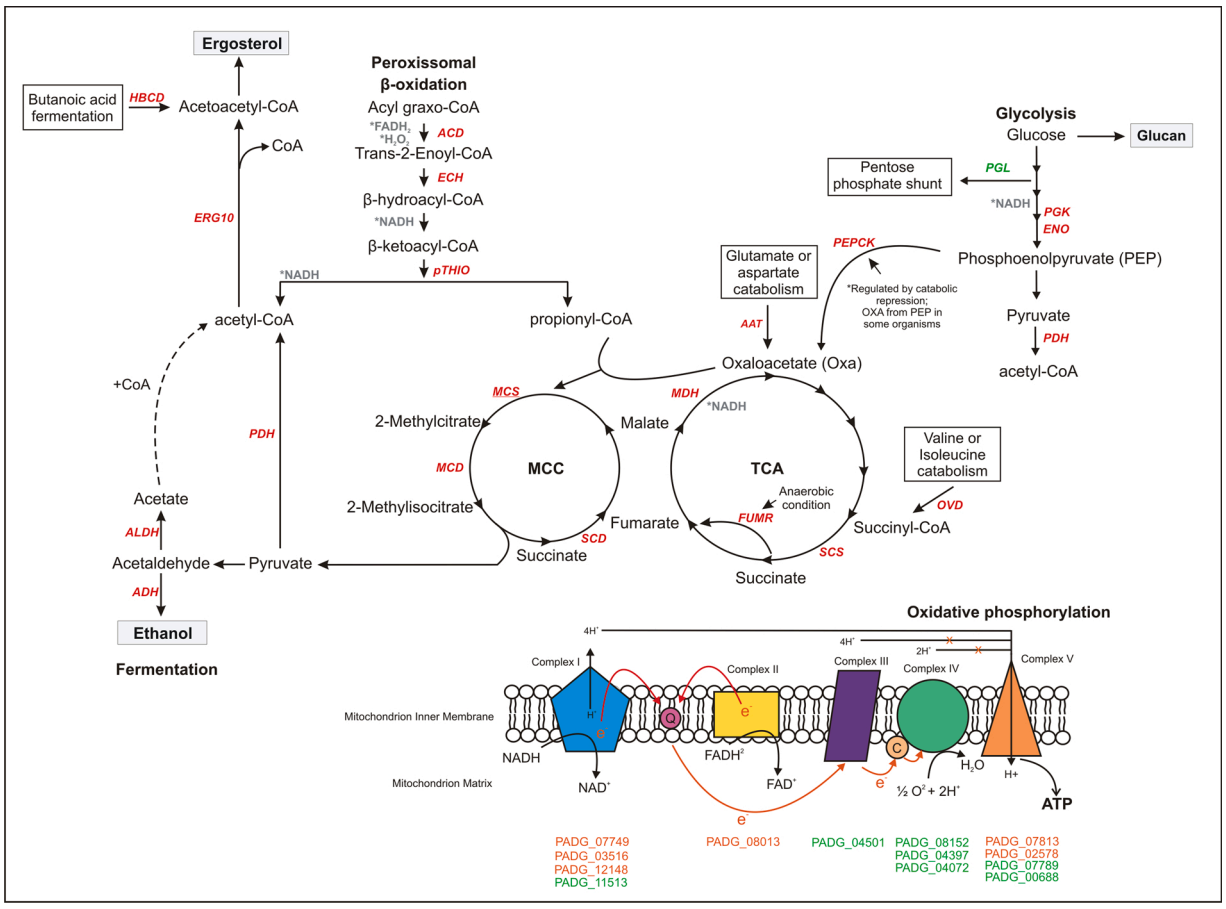

Fig. 1. Overview of the metabolic responses of *P. brasiliensis* to hypoxia. The figure summarizes data from proteomic analyses and suggests the modulation of the energy metabolism by *P. brasiliensis* to compensate hypoxia at 12 h of stress. Red or green indicate up or down regulated proteins, respectively. Proteins are demonstrated using abbreviations and accession numbers (oxidative phosphorylation pathway, e.g.). Underline indicates proteins that were also confirmed by biochemical assays. Gray boxes indicate molecules which were also analyzed by other procedures, validating the proteome data (ethanol, ergosterol and glucan). Asterisks and gray letters demonstrate products related to chemical reactions from proteins detected in our analysis (NADH, H_2O_2 and $FADH_2$). Dashed line indicates a suggested metabolic process to acetyl-CoA production from acetate (done by acetyl-CoA synthetase enzyme, not detected in our study). **HBCD:** 3-hydroxybutyryl-CoA dehydrogenase - PADG_01228; **ERG10:** Acetyl-CoA C-acetyltransferase - PADG_02751; **ALDH:** Aldehyde dehydrogenase - PADG_05081; **ADH:** Alcohol dehydrogenase 1 - PADG_11405; **PDH:** complex of pyruvate dehydrogenase → Pyruvate dehydrogenase kinase 2/3/4 - PADG_12250, Dihydrolipoamide acetyltransferase - PADG_07213 and Dihydrolipoyl dehydrogenase - PADG_06494; **ACD:** Acyl-CoA dehydrogenase - PADG_06805; **ECH:** Enoyl-CoA hydratase - PADG_01209; **pTHIO:** Peroxisomal 3-ketoacyl-CoA thiolase - PADG_03194; **MCS:** Methylcitrate synthase; **MCD:** 2-methylcitrate dehydratase - PADG_04718; **SCS:** Succinyl-CoA synthetase alpha subunit - PADG_02260; **SCD:** Succinate dehydrogenase [ubiquinone] iron-sulfur subunit - PADG_08013; **FUMR:** Fumarate reductase (NADH) - PADG_02592; **MDH:** Malate dehydrogenase, NAD-dependent - PADG_07210; **AAT:** Aspartate aminotransferase - PADG_01621; **OVD:** 2-oxoisovalerate dehydrogenase subunit alpha - PADG_03514; **PEPCK:** Phosphoenolpyruvate carboxykinase - PADG_08503; **ENO:** Enolase - PADG_04059; **PGK:** Phosphoglycerate kinase - PADG_01896; **PGL:** 6-phosphogluconolactonase - PADG_07771. **Oxidative phosphorylation chain → Complex I:** PADG_07749 - NAD(P)H:quinone oxidoreductase, type IV; PADG_03516 - NADH dehydrogenase (ubiquinone) Fe-S protein 3; PADG_12148 - NADH-ubiquinone oxidoreductase 78 kDa subunit, mitochondrial; PADG_11513 - NADH-ubiquinone oxidoreductase; **Complex II:** PADG_08013 - Succinate dehydrogenase [ubiquinone] iron-sulfur subunit, mitochondrial; **Complex III:** PADG_04501 - Ubiquinol-cytochrome c reductase subunit 7; **Complex IV:** PADG_08152 - Cytochrome c oxidase assembly factor 6; PADG_04397 - Cytochrome c oxidase subunit 4, mitochondrial; PADG_04072 - Cytochrome c oxidase-assembly factor COX23, mitochondrial; **Complex V:** PADG_07813 - ATP synthase F1, gamma subunit; PADG_02578 - ATP synthase subunit 4, mitochondrial; PADG_07789 - ATP synthase subunit delta, mitochondrial; and PADG_00688 - F-type H+-transporting ATPase subunit h.

enzyme is regulated by catabolite repression by cAMP and glucose, inhibiting gluconeogenesis when glucose and other carbohydrates are available (Goldie, 1984). Interesting, in some organisms such as *Dipetalonema viteae*, a parasitic nematode, and also in *Trypanosoma cruzi*, the parasitic flagellate, the PEPCK was detected as a non-canonical enzyme forming OXA from PEP, which in turn enters the citric acid cycle (Christie et al., 1987; Cymeryng et al., 1995). In *T. cruzi*, when glucose is in excess, in epimastigotes grown in axenic culture, the carboxylation of PEP is favored, leading to succinate excretion with concomitant NADH re-oxidation (Cazzulo, 1992). In this sense, we believe that glycolysis is activated. In fact, *P. brasiliensis* yeast cells submitted to hypoxia and normoxia until 48 h similarly consume glucose (Supplementary Fig. 4). In addition, the down-regulation of the 6-phosphogluconolactonase (PADG_07771) enzyme from pentose phosphate shunt, reinforces the suggestion of the carbon flux flowing to pyruvate production (Table S4, Fig. 1). In turn, pyruvate produces acetyl-CoA supported by the pyruvate dehydrogenase complex: pyruvate dehydrogenase kinase 2/3/4 (PADG_12250), dihydrolipoamide acetyltransferase (PADG_07213) and dihydrolipoyl dehydrogenase (PADG_06494) (Table S3; Fig. 1). We believe that glycolysis supplies part of the energy to the cell, but not in sufficient quantities, requiring other alternative pathways to supply sufficient energy. This hypothesis is supported by the activation of the breakdown of lipids and amino acids during infection, and consequently activation of pathways such as beta-oxidation and glyoxylate cycle (Parente-Rocha et al., 2015; Pigosso et al., 2017).

We also suggest that glucose from culture medium can be an

important precursor of some components of the cell wall such as glucan (Sorais et al., 2010) produced in higher amounts during hypoxia (Fig. 2A). On the contrary, the amount of chitin, another component of the cell wall, has not changed (Fig. 2B). The increase in glucans has also been found in copper deprivation (Petito et al., 2020), osmotic adaptation (Rodrigues et al., 2016) and during infection in alveolar macrophages (Chaves et al., 2019). It is known that β-glucan is an excellent pathogen associated molecular patterns (PAMP) recognized by macrophages and neutrophils, activating Dectin-1 and TLR2, increasing the effectiveness of the immune response against the pathogen (Brown et al., 2002; Gantner et al., 2003; Shepardson et al., 2013). In counterpart, outer layer α-glucan prevents recognition abrogating the immune response (Rappleye et al., 2007, 2004; San-Blas et al., 1977). Idem it is known that in *A. fumigatus* hypoxia-driven cell wall changes results in an increase of β-glucan content, leading to high macrophage and neutrophil inflammatory responses that are largely dependent on Dectin-1 signaling (Shepardson et al., 2013). Likewise, in *P. brasiliensis* we detected hypoxia-induced β-glucan increase using an aniline blue dye (Fig. 2A), specific for β-glucan (de Curcio et al., 2017). Thus, the data suggest that the hypoxic environments found in the host infection milieu could result in activation of the immune response against *Paracoccidioides* spp.

3.1.2. Ergosterol synthesis increases in yeast cells in hypoxia

Regarding beta-oxidation, three specific enzymes were up-regulated resulting in the production of acetyl-CoA and propionyl-CoA (Table S3, Fig. 1). The enzymes acyl-CoA dehydrogenase (PADG_06805), enoyl-CoA hydratase (PADG_01209) participate in mitochondrial and peroxisomal beta-oxidation. Interesting, a specific peroxisomal beta-oxidation enzyme, 3-ketoacyl-CoA thiolase (PADG_03194), was up-regulated (Table S3, Fig. 1). The results suggest that peroxisomal beta-oxidation is activated and, as consequence, products such as acetyl-CoA and propionyl-CoA are obtained. The evidence is that acetyl-CoA is also produced from pyruvate metabolism since the pyruvate dehydrogenase complex was also up-regulated (Table S3, Fig. 1). Furthermore, NADH and $FADH_2$ from beta-oxidation provides energy during oxidative phosphorylation, discussed below.

Acetyl-CoA probably is feeding ergosterol synthesis in *P. brasiliensis* facing hypoxia (Fig. 1). The enzyme acetyl-CoA C-acetyltransferase (PADG_02751) was up-regulated (Table S3). This enzyme is also named as Erg10 and catalyzes the formation of acetoacetyl-CoA in the biosynthesis of mevalonate, an intermediate required for the biosynthesis of sterols and nonsterol isoprenoids (Karst and Lacroute, 1977). Also, other pathways feeding acetoacetyl-CoA production from butanoic acid fermentation could occur (Taylor et al., 2010) reinforcing the high level of expression of 3-hydroxybutyryl-CoA dehydrogenase (PADG_01228) (Table S3). Probably, acetoacetyl-CoA is directed towards the production of ergosterol, necessary for the adaptation of *Pb*18 to hypoxia. In fact, data here provided demonstrated that *P. brasiliensis* increases the amount of ergosterol during hypoxia (Fig. 3A). In fungi such as *Candida*

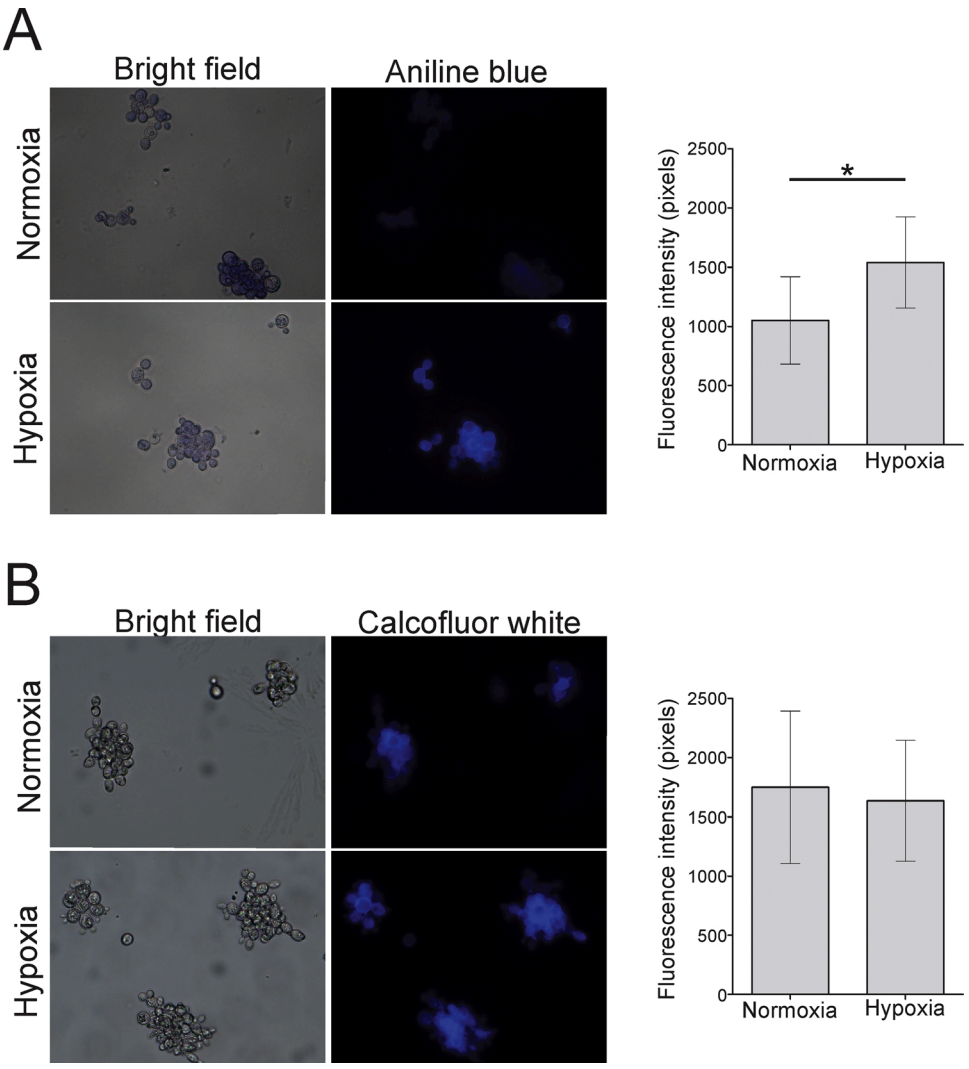

Fig. 2. Content of cell wall polymers of *P. brasiliensis* in normoxia and hypoxia. (A) The glucan content was evaluated using Aniline blue as a dye. **(B)** The chitin content was evaluated using Calcofluor white as a dye. Cells were grown at 36 °C and cultivated in normoxia and hypoxia for 12 h in biological triplicate. Digital images acquired using Axio-Scope A1 microscope. The fluorescence intensity (in pixels) of the stained cells was measured using the AxioVision software (Carl Zeiss, Germany). The mean values of fluorescence intensity and the standard deviation of each analysis were used to plot graph (right). "*" indicates p-values ≤ 0.05 by Student's *t*-test. All images were obtained in magnification of 400 × .

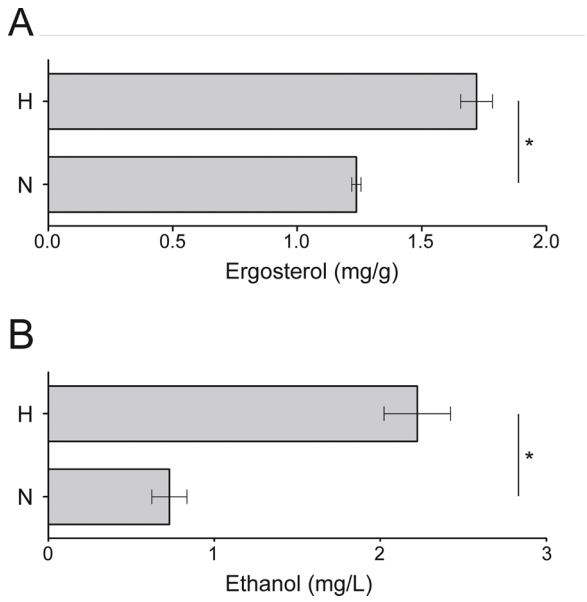

Fig. 3. Confirmatory biochemistry tests. Total intracellular sterols and ethanol were measured from *Paracoccidioides brasiliensis*, strain 18 (ATCC 32069), all in biological triplicates. Cells were grown in BHI liquid medium at 36 °C and cultivated in normoxia and hypoxia for 12 h. **(A) Ergosterol dosage**. The wet weight of the cell pellet was determined for each replicate and condition. The heptane layer (containing ergosterol) was obtained and the ergosterol content was determined by a percentage of the wet cell weight calculated by the following equations: value 1 = $[(A_{281.5}/290) \times F]$/wet cell weight, value 2 = $[(A_{230}/518) \times F]$/wet cell weight. The percent of ergosterol is calculated as follow: value 1 - value 2. "F" is the factor for dilution and 290 and 518 are fixed values determined for crystaline ergosterol and dihydroergosterol, respectively. **(B) Ethanol dosage**. The intracellular ethanol concentration was measured based in NADH quantification that is released after the oxidation of ethanol to acetaldehyde followed by oxidation of acetaldehyde to acetic acid. A total of 10^8 *P. brasiliensis* yeast cells was recovered at 12 h of normoxia and hypoxia in biological triplicates. The mean ± standard deviation (error bars) were shown and "*" indicates the results statistically significant at p-values ≤ 0.05 by Student's *t*-test. **N**: normoxia; **H**: hypoxia.

albicans, *C. neoformans*, *A. fumigatus* and *Aspergillus nidulans*, fatty acids and ergosterol metabolism are increased in response to hypoxia and is clear that ergosterol is important to stability, fluidity and structure of the fungi plasma membrane (Askew et al., 2009; Barker et al., 2012; Chun et al., 2007; Lee et al., 2007; Setiadi et al., 2006; Shimizu et al., 2009). So, it is possible that ergosterol is important to compensate negative effects in *P. brasiliensis* cellular membrane during hypoxia.

Due to its properties, ergosterol is known to be the target of the majority of clinically available antifungals (Bhattacharya et al., 2018; Dhingra and Cramer, 2017), and it is also relevant for pathogenesis of *P. brasiliensis*. Furthermore, ergosterol is an immunoactive fungal molecule (Koselny et al., 2018; Rodrigues, 2018) which can trigger macrophage pyroptosis when infected by *S. cerevisiae*, *C. albicans*, *C. neoformans* and *P. brasiliensis* (Ketelut-Carneiro et al., 2015; Koselny et al., 2018; Uwamahoro et al., 2014; Wellington et al., 2014). Pyroptosis is an inflammatory mode of programmed cell death mediated by the activation of the inflammasome, resulting in lysis of the cell membrane (Bauernfeind and Hornung, 2013; Liu and Lieberman, 2017). The link between ergosterol and pyroptosis has been demonstrated in *C. albicans* because the key transcriptional regulator of ergosterol biosynthesis, Upc2, was necessary for induction of the pyroptosis (Wellington et al., 2014). In addition, fungal sterol, by avoiding be limited to the plasma membrane, has a wide distribution in fungal cell, as well is detected in extracellular vesicles suggesting immunological functions (Rodrigues, 2018; Rodrigues et al., 2007). Together, our findings on the content of hypoxia and ergosterol highlight the importance of this lipid for the adaptation to *P. brasiliensis* hypoxia.

3.1.3. The methylcitrate cycle is activated in yeast cells submitted to hypoxia

Pyruvate is a key intermediate in several metabolic pathways; since glycolysis is decreased, it is possible that pyruvate synthesis in *P. brasiliensis* submitted to 12 h of hypoxia relies in the tricarboxylic acid (TCA) and methylcitrate cycles (Fig. 1). In fact, propionyl-CoA can condense with oxaloacetate for the activation of the methylcitrate cycle (MCC), producing pyruvate (Brock et al., 2000). Regarding the TCA cycle, four enzymes were increased: succinyl-CoA synthetase (PADG_02266), succinate dehydrogenase (PADG_08013), fumarate reductase - NADH (PADG_02592) and malate dehydrogenase (PADG_07210) (Table S3, Fig. 1). Notice that succinate dehydrogenase (PADG_08013) can also act in MCC and oxidative phosphorylation processes (Complex II). Even more, fumarate reductase - NADH (PADG_02592) is, in anaerobic conditions, an enzyme that produces fumarate from succinate (Tielens and Van Hellemond, 1998) and was induced in *Saccharomyces cerevisiae* during anaerobiosis (Camarasa et al., 2007).

The activation of the MCC could occur given that 2-methylcitrate dehydratase (PADG_04718) was up-regulated in *Pb*18 under hypoxia (Table S1, Fig. 1). This enzyme catalyzes the second step of the MCC (Brock et al., 2000). In addition, the specific activity of methylcitrate synthase (MCS), was increased in yeast cells in hypoxia, as depicted in Fig. 4A. It is a MCC specific enzyme and promotes the condensation of propionyl-CoA with oxaloacetate (Brock et al., 2000; Brock and Buckel, 2004; Santos et al., 2020). One of the products from MCC is pyruvate, reinforcing all suggested carbon flux (Fig. 1). Lastly, the enzymes from amino acid catabolism aspartate aminotransferase (PADG_01621) and 2-oxoisovalerate dehydrogenase (PADG_03514) support the formation of oxaloacetate (Verleur et al., 1997) and succinyl-CoA (Zhang et al., 2017), respectively (Table S3). Interestingly, during lung infection in murine the glyoxylate cycle was activated (Pigosso et al., 2017), while in alveolar macrophages the MCC is activated (Chaves et al., 2019). This finding reveals the plasticity of *Paracoccidioides* spp. in adapting and surviving critical situations.

3.1.4. The production of ethanol is high in yeast cells in hypoxia

Acetaldehyde is produced from pyruvate in a non-oxidative decarboxylation by pyruvate decarboxylase, releasing carbon dioxide. Acetaldehyde, in turn, could be converted to ethanol catalyzed by alcohol dehydrogenase (Eram and Ma, 2013; Nelson and Cox, 2014) or in acetate by aldehyde dehydrogenase (PADG_05081). In this study, alcohol dehydrogenase 1 (PADG_11405) increased in *P. brasiliensis* in hypoxia (Table S3). To validate proteomic data, ethanol dosage was carried out and in fact there is a significantly higher level of ethanol in *P. brasiliensis* yeast cells submitted to hypoxia compared to normoxia (Fig. 3B). Ethanol metabolism was previously described in *Paracoccidioides* species (Araújo et al., 2019; Felipe et al., 2005; Lima et al., 2014; Pigosso et al., 2013; Rezende et al., 2011) and this metabolite has also been described as relevant to the pathogenicity of *A. fumigatus* (Barker et al., 2012; Grahl et al., 2011; Teutschbein et al., 2010) and *P. brasiliensis* (Parente-Rocha et al., 2015; Pigosso et al., 2017). Related to acetate, aldehyde dehydrogenase (PADG_05081) was also up-regulated (Table S1). Aldehyde dehydrogenases are a group of enzymes that catalyze the oxidation of aldehydes converting them to carboxylic acids, using oxygen from water (Marchitti et al., 2008). In this sense, aldehyde dehydrogenase from *P. brasiliensis* probably is producing acetate from acetaldehyde (Fig. 1). Possibly, ethanol and acetate can be also used as alternative carbon (Fig. 1). Previous study confirms that acetate is used by different species of the *Paracoccidioides* complex (Baeza et al., 2017).

3.1.5. Oxidative phosphorylation chain is affected during hypoxia

The oxidative phosphorylation chain had representative enzymes detected in this study (a total of thirteen). Some of them had increased

whereas other reduced levels of expression in *P. brasiliensis* in 12 h of hypoxia (Table S3 and S4). Fig. 1 depicted each one related to its respective complex (Complex I, II, III, IV or ATP Synthase Complex) with its respective nomenclatures in the legend. The results show that the complexes are affected, mainly complex IV, causing a loss in electron transport (Tables S3 and S4, Fig. 1). The structure and functionality of mitochondria were analyzed in this study (Fig. 5). Fluorescence microscopy analysis using MitoTracker dye showed that the structure of mitochondria during hypoxia is not affected (Fig. 5A). On the other hand, the mitochondrial electric potential was affected by hypoxia (Fig. 5B). Rhodamine is a permeable lipophilic cationic fluorescent probe that accumulates in mitochondria and is distributed into the mitochondrial matrix in response to mitochondrial electric potential (Baracca et al., 2003; Tupe et al., 2015). Further, it is notable that those identified proteins of complex IV are all down-regulated, especially cytochrome c complex (Fig. 1). Thus, cytochrome c oxidase activity was investigated to validate the functionality of complex IV (Fig. 4B). As result, the amount of reduced ferrocytochrome C is higher in hypoxia due absence of cytochrome c oxidase activity. Cytochrome c oxidase reduces molecular oxygen in a reaction coupled with a proton pumping process (Tsukihara et al., 1995). Data indicate that mitochondrial reactions are affected by hypoxia. In summary, cellular energy is providing partly by glycolysis and partly by oxidative phosphorylation.

3.1.6. Nitrogen metabolism changes during hypoxia

Formamidase (PADG_06490) and oxireductase 2-nitropropane dioxygenase (PADG_00446) were increased during hypoxia of yeast cells. Nitrogen metabolism involves chemical reactions and pathways that metabolize organic and inorganic compounds (Nelson and Cox, 2014). To validate data, formamidase enzymatic activity was evaluated demonstrating that this enzyme presented high activity in *Pb*18 in hypoxia (Fig. 4C). Formamidase hydrolyzes formamide to produce ammonia and formate (Skouloubris et al., 1997) and plays a role in fungal nitrogen metabolism (Borges et al., 2005; Felipe et al., 2005; Fraser et al., 2001). In *Paracoccidioides*, formamidase was associated with the cell wall (Borges et al., 2010) and secreted (de Oliveira et al., 2018) mainly in the mycelial/infective phase of the fungus (Weber et al., 2012). Still in this fungus, formamidase is recognized by sera from patients with paracoccidioidomycosis (Borges et al., 2005) and was highly expressed during mice lung infection (Pigosso et al., 2017).

3.1.7. Defense against H_2O_2 changes during hypoxia

Peroxisomal beta-oxidation could generate hydrogen peroxide (Nelson and Cox, 2014). Peroxiredoxin (PADG_04912) was increased in yeast cells in hypoxia (Table S3). This enzyme is a peroxidase that can reduce hydroperoxides and is a cytoprotective antioxidant enzyme acting against endogenous or exogenous peroxide attacks (Knoops et al., 2011). Other peroxiredoxins are thiol specific antioxidant (TSA) and thioredoxin peroxidase (TPx) (Chae and Rhee, 1994). These enzymes share the same basic catalytic mechanism in which a redox active site is oxidized to a sulfenic acid by the peroxide substrate (Claiborne et al., 1999). In this sense, we performed a dosage of reduced thiol from normoxia and hypoxia protein samples; organosulfur compound is more reduced in hypoxia than normoxia (Fig. 6). Additionally, the mitochondrial response against oxidative stress could be due to cytochrome c peroxidase - PADG_03163 (Fig. 6), while superoxide dismutase [Cu-Zn] (PADG_07418) and glutathione peroxidase (PADG_04587) are down-regulated (Fig. 6). Notably, disulfide-isomerase (PADG_03841) also increased (Fig. 6). The activity of such proteins enables the process of cellular detoxification generated by the metabolic processes during hypoxia. Similarly, defense against oxidative stress is mediated by cytochrome c peroxidase and thioredoxins during infection (Chaves et al., 2019; Parente-Rocha et al., 2015; Pigosso et al., 2017), and the presence of CCP is essential for the establishment of the infection (Parente-Rocha et al., 2015).

3.2. P. brasiliensis versus P. lutzii proteome comparison in hypoxia

To depict similarities and differences related to hypoxia responses between *Paracoccidioides* species, data from a previous study were used (Table 1). Hypoxia was first described in *P. lutzii* species (Lima et al., 2015); in this work we used *P. brasiliensis*. Here, peptides from normoxia and hypoxia were obtained and samples were iTRAQ-labeled, as previously performed (Queiroz et al., 2014), while for *P. lutzii* large scale quantitative data were obtained using a label free proteomic technique, NanoUPLC-MS^E (Murad and Rech, 2012).

Lima and collaborators (2015) depicted the hypoxia responses from *P. lutzii* in 12 and 24 h of hypoxia, compared with normoxia. Here, the proteomic approach was performed in *P. brasiliensis* in 12 h of hypoxia. In total, 216 differentially expressed proteins were obtained. On the other hand, 134 and 154 differentially expressed proteins were obtained in *P. lutzii*, in 12 and 24 h in hypoxia, respectively (Lima et al., 2015). Some biological categories presented similarities related to up or down-regulation of proteins during hypoxia responses in *P. lutzii* and *P. brasiliensis* (Table 1). Enzymes from glycolysis were up-regulated in *P. brasiliensis* (Table S3); in *P. lutzii*, glycolysis was up-regulated only in 24 h (Lima et al., 2015). In *P. brasiliensis,* glycolysis is feeding oxaloacetate and pyruvate amounts (probably precursor to acetyl-CoA and ethanol) (Fig. 1). In *P. lutzii*, glycolysis was activated after 24 h of low oxygen stress. The pentose-phosphate pathway, for example, was down

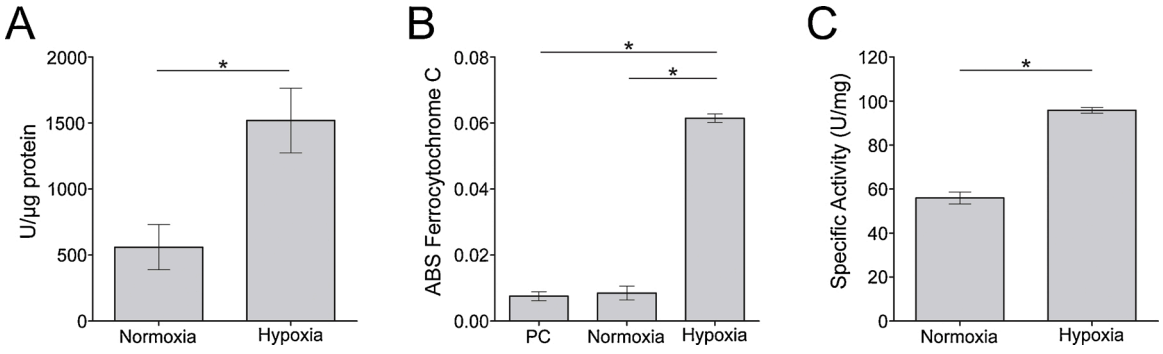

Fig. 4. Enzymatic assays. Protein extracts from *Pb*18 in normoxia and hypoxia grown at 36 °C, for 12 h in biological triplicates. **(A) Methylcitrate synthase activity.** The condensation of propionyl-CoA with oxaloacetate was measured by the production of CoASH read at 412 nm at 25 °C. One unit of enzyme activity was defined as the amount of enzyme producing 1 µmol min^{-1} of CoASH under the assay conditions. **(B) Cytochrome c oxidase activity.** The reduced ferrocytochrome C as measured at 550 nm. The positive control (PC) and normoxia reveals a decrease of reduced ferrocytochrome C absorbance due to oxidation by cytochrome c oxidase. **(C) Formamidase activity.** The formamidase activity was determined by amount of ammonia released for each sample. One unit (U) of formamidase specific activity was defined as the amount of enzyme required to hydrolyze 1 µmol of formamide (corresponding to the formation of 1 µmol of ammonia) per min per mg of total protein. The mean ± standard deviation (error bars) were shown and "*" indicates the results statistically significant at p-values ≤ 0.01 by Student's *t*-test.

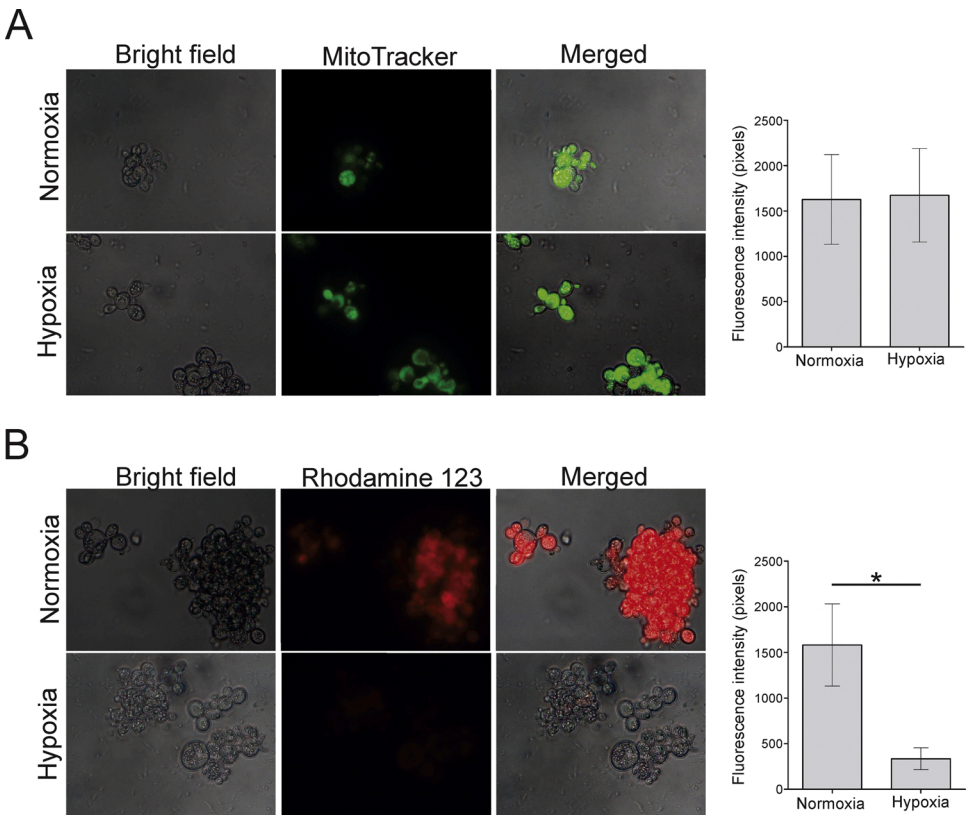

Fig. 5. Mitochondrial integrity and activity of *P. brasiliensis* submitted to normoxia and hypoxia. (A) The mitochondrial integrity was evaluated by using MitoTracker Green FM as a dye for mitochondrial structural integrity. **(B)** The mitochondrial activity was evaluated by using Rhodamine 123 as a dye for mitochondrial membrane potential. Cells were grown at 36 °C and cultivated in normoxia and hypoxia for 12 h in biological triplicate. Digital images acquired using Axio-Scope A1 microscope. The fluorescence intensity (in pixels) of the stained cells was measured using the AxioVision software (Carl Zeiss, Germany). The mean values of fluorescence intensity and the standard deviation of each analysis were used to plot graph (right). "*" indicates p-values ≤ 0.01 by Student's *t*-test. All images were obtained in magnification of 400 × .

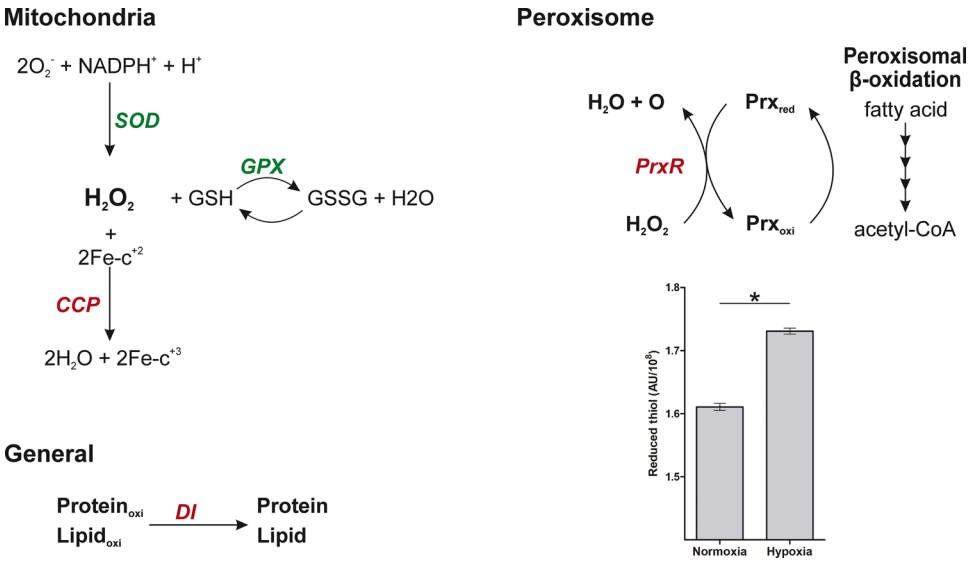

Fig. 6. Overview of detoxification mechanisms against oxidative stress in *P. brasiliensis* submitted to hypoxia. The figure summarizes data from proteomic analyses and suggests the mechanisms used by the fungus to counteract oxidative stress generated by hypoxia. Red or green indicate up or down regulated proteins, respectively. SOD: superoxide dismutase - PADG_07418, GPX: glutathione peroxidase - PADG_04587, CCP: cytochrome c peroxidase - PADG_03163, DI: disulfide isomerase - PADG_03841, PrxR: peroxiredoxin - PADG_04912. The reduced thiol level was measured in *Pb*18 yeast cells submitted to normoxia and hypoxia in biological triplicate. The mean values (in pixels) and the standard deviation of each analysis were used to plot graph (right). "*" indicates p-values ≤ 0.05 by Student's *t*-test.

regulated in both studies while amino acid and lipid metabolisms were up-regulated (Table 1). Also, acetyl-CoA, pyruvate and ergosterol synthesis were increased in both fungi submitted to hypoxia. In both, acetyl-CoA comes mainly from beta-oxidation and acetaldehyde catabolism, not from pyruvate. Further, ergosterol synthesis is mediated by acetoacetyl-CoA production (Tables 1, S3 and S4; Fig. 1; Lima et al., 2015). Oxidative phosphorylation chain was also impaired in both fungi during hypoxia (Table S3 and S4), as confirmed using fluorescence assays (Fig. 5; Lima et al., 2015). Probably, impaired electron transport affects the mitochondria ATP yield.

Comparing *Paracoccidioides* species facing hypoxia, differences were also depicted. Part of the tricarboxylic cycle (TCA) enzymes were up-regulated in *P. brasiliensis* (Tables 1 and S1) but not in *P. lutzii* (Lima et al., 2015). For many organisms, exposure to hypoxia results in decreased flux through the TCA cycle concomitant with a decrease in aerobic respiration (Synnott et al., 2010; Todd et al., 2006). Some biological categories were changed only in *P. brasiliensis* such as methylcitrate cycle (MCC) and those involved with acetate and ethanol synthesis, all of them up regulated (Tables 1 and S3). The MCC as well as TCA produce precursors to other biochemical routes including those related with acetate and ethanol synthesis (Fig. 1). These categories were not detected in *P. lutzii* facing hypoxia (Lima et al., 2015).

Table 1
Comparative analysis of proteome between P. lutzii and P. brasiliensis submitted to hypoxia.

Biological process	*Paracoccidioides* species (isolate)	
	P. lutzii (*Pl*01)[a]	*P. brasiliensis* (*Pb*18)[b]
Glycolysis (specific enzyme)	Down / Up	Up
Gluconeogenesis (specific enzyme)	# / #	Up
Pentose-phosphate pathway	Down/ Down	Down
Tricarboxylicacid cycle (TCA)	Down/ Down	Up
Methylcitrate cycle (MCC)	# / #	Up
Oxidative phosphorylation chain	Down (Complexes I, IV and V) /Up (Complex V)	Up (Complexes I, II and V) Down (Complexes III, IV and V)
Amino acid metabolism	Up/ Up	Up
Lipid, fatty acid and isoprenoid metabolism	Up/ Up	Up
Secondary metabolism	Up/?	Down
Acetyl-CoA synthesis	Up/ Up	Up
Pyruvate synthesis	# / Up	Up
Acetate synthesis	# / #	Up
Ethanol (fermentation) synthesis	# / #	Up
Ergosterol synthesis	# / Up	Up
GABA shunt	# / Up	#
Cell cycle and DNA process	Down / Up	Down
Transcription	?/ Up	Down
Translation	Up/ Up	Up
Protein fate and degradation	Up/ Up	Down
Cellular transport	? / Up	Down
Signal transduction	Up/ #	Down
Cell rescue, defense and virulence	Up/ Up	Up and Down (According to the biological process)

#: No enzymes related to the biological process or chemical reactions were detected by proteome.
?: No conclusive data from proteomic studies.
[a] Proteome obtained from *Paracoccidioides lutzii* (*Pl*01) facing hypoxia for 12 and 24 h (Lima et al., 2015), separated by bars, respectively.
[b] Proteome obtained from *Paracoccidioides brasiliensis* (*Pb*18) facing hypoxia for 12 h (this study).

Proteins from GABA shunt were not detected in *P. brasiliensis* in 12 h of hypoxia and were increased in *P. lutzii* in 24 h of this stress (Lima et al., 2015). The γ-aminobutyric acid (GABA) is generated from glutamate (Schousboe and Waagepetersen, 2007) and produces succinate (via GABA shunt) which in turns can enters in the tricarboxylic acid cycle (TCA) (Aoki et al., 2003; Yadav et al., 2011). In fact, the GABA shunt is described as an alternative route to the TCA cycle (Masuo et al., 2010) helping organisms to avoid accumulation of high NADH levels in the absence of a terminal electron acceptor such as oxygen (Barker et al., 2012).

The comparison between *P. brasiliensis* and *P. lutzii* submitted to hypoxia can contribute with studies involving metabolic differences in members of the *Paracoccidioides* complex. Using proteome, metabolic differences were detected among members of *Paracoccidioides* genus. Proteins related to gluconeogenesis, glyoxylic/glyoxylate cycle, TCA and respiratory chain, ethanol synthesis,β-oxidation and methylcitrate cycle categories were detected as differentially regulated (Baeza et al., 2017; Pigosso et al., 2013). Metabolic particularities were also detected when comparing virulence among *P. brasiliensis* isolates (do Amaral et al., 2019). The analysis indicate that highly virulent isolates probably expressed a higher amount of phosphoglycerate kinase and glyceraldehyde-3-phosphate dehydrogenase than isolates of low virulence, for example (do Amaral et al., 2019). Interesting, our data indicate that *P. brasiliensis*, *Pb*18, also increases the expression of phosphoglycerate kinase during hypoxia while *P. lutzii*, *Pl*01, not (Lima et al., 2015). In fact, the diversity of metabolic responses found between the two species probably reflects in their pathogenicity (do Amaral et al., 2019; Marcos et al., 2014; Siqueira et al., 2016). Altogether, these metabolic differences could be important to define particularities of *Paracoccidioides* spp. in future.

4. Conclusion

In this research, we have studied the hypoxic adaptation of *P. brasiliensis* by iTRAQ-labelling proteomic and biochemical analyses. Results revealed that *P. brasiliensis* supports low oxygen tensions, reprogramming its metabolism; glycolysis is increased, and pentose-phosphate pathway is not active. Pyruvate is formed from glycolysis and methylcitrate cycle and converted to ethanol and acetate. Oxidative phosphorylation chain is deficient. The membrane and cell wall are modified by the accumulation of ergosterol and glucan, respectively. Cell cycle and core processes are downregulated. Some responses are different between species in the *Paracoccidioides* genus. Proteome comparisons between *P. brasiliensis* and *P. lutzii* show us that both have metabolic particularities during hypoxia adaptation. Particularly, GABA shunt increases were detected only in *P. lutzii*, while methylcitrate cycle (MCC) only in *P. brasiliensis*. Lipid metabolism, ergosterol synthesis and oxidative phosphorylation chain have identical patterns between species. The effect of differential protein expression in species during infection needs to be further evaluated. The purpose of our work was to provide basic protein data to support studies of host pathogen interaction in laboratory models of infection in not-so-distant future.

Declaration of Competing Interest

The authors declare that the research was conducted in the absence of any commercial or financial relationships that could be construed as a potential conflict of interest.

CRediT authorship contribution statement

Lucas Nojosa Oliveira: Conceptualization, Methodology, Software, Formal analysis, Validation, Investigation, Writing - original draft, Writing - review & editing. **Patrícia de Sousa Lima:** Methodology, Formal analysis, Validation, Investigation, Writing - original draft, Writing - review & editing. **Danielle Silva Araújo:** Methodology, Validation. **Igor Godinho Portis:** Methodology, Validation. **Agenor de Castro Moreira dos Santos Júnior:** Methodology, Validation, Investigation. **Alexandre Siqueira Guedes Coelho:** Software, Formal analysis, Data curation. **Marcelo Valle de Sousa:** Data curation. **Carlos André Ornelas Ricart:** Data curation. **Wagner Fontes:** Software, Formal analysis, Data curation. **Célia Maria de Almeida Soares:** Conceptualization, Data curation, Funding acquisition, Resources, Project administration, Supervision, Writing - original draft, Writing - review & editing.

Acknowledgement

This work was supported by grants from Instituto Nacional de Ciência e Tecnologia de Estratégias de Interação Patógeno-Hospedeiro - Fundação de Amparo à Pesquisa do Estado de Goiás (FAPEG).

Appendix A. Supplementary data

Supplementary material related to this article can be found, in the online version, at doi:https://doi.org/10.1016/j.micres.2021.126730.

References

Aoki, H., Uda, I., Tagami, K., Furuya, Y., Endo, Y., Fujimoto, K., 2003. The production of a new tempeh-like fermented soybean containing a high level of gamma-aminobutyric acid by anaerobic incubation with Rhizopus. Biosci. Biotechnol. Biochem. 67, 1018–1023. https://doi.org/10.1271/bbb.67.1018.

Araújo, D.S., Pereira, M., Portis, I.G., dos Santos Junior, Ade C.M., Fontes, W., de Sousa, M.V., Assunção, Ldo P., Baeza, L.C., Bailão, A.M., Ricart, C.A.O., Brock, M., Soares, C.Mde A., 2019. Metabolic peculiarities of *Paracoccidioides brasiliensis* dimorphism as demonstrated by iTRAQ labeling proteomics. Front. Microbiol. 10 https://doi.org/10.3389/fmicb.2019.00555.

Arthington-Skaggs, B.A., Jradi, H., Desai, T., Morrison, C.J., 1999. Quantitation of ergosterol content: novel method for determination of fluconazole susceptibility of *Candida albicans*. J. Clin. Microbiol. 37, 3332–3337.

Askew, C., Sellam, A., Epp, E., Hogues, H., Mullick, A., Nantel, A., Whiteway, M., 2009. Transcriptional regulation of carbohydrate metabolism in the human pathogen *Candida albicans*. PLoS Pathog. 5, e1000612 https://doi.org/10.1371/journal.ppat.1000612.

Baeza, L.C., da Mata, F.R., Pigosso, L.L., Pereira, M., de Souza, G.H.M.F., Coelho, A.S.G., de Almeida Soares, C.M., 2017. Differential metabolism of a two-carbon substrate by members of the *Paracoccidioides genus*. Front. Microbiol. 8 https://doi.org/10.3389/fmicb.2017.02308.

Baracca, A., Sgarbi, G., Solaini, G., Lenaz, G., 2003. Rhodamine 123 as a probe of mitochondrial membrane potential: evaluation of proton flux through F(0) during ATP synthesis. Biochim. Biophys. Acta 1606, 137–146.

Barker, B.M., Kroll, K., Vödisch, M., Mazurie, A., Kniemeyer, O., Cramer, R.A., 2012. Transcriptomic and proteomic analyses of the *Aspergillus fumigatus* hypoxia response using an oxygen-controlled fermenter. BMC Genomics 13, 62. https://doi.org/10.1186/1471-2164-13-62.

Bauernfeind, F., Hornung, V., 2013. Of inflammasomes and pathogens – sensing of microbes by the inflammasome. EMBO Mol. Med. 5, 814–826. https://doi.org/10.1002/emmm.201201771.

Bhattacharya, S., Esquivel, B.D., White, T.C., 2018. Overexpression or deletion of ergosterol biosynthesis genes alters doubling time, response to stress agents, and drug susceptibility in *Saccharomyces cerevisiae*. mBio 9. https://doi.org/10.1128/mBio.01291-18.

Borges, C.L., Pereira, M., Felipe, M.S.S., de Faria, F.P., Gomez, F.J., Deepe, G.S., Soares, C.M.A., 2005. The antigenic and catalytically active formamidase of *Paracoccidioides brasiliensis*: protein characterization, cDNA and gene cloning, heterologous expression and functional analysis of the recombinant protein. Microbes Infect. 7, 66–77. https://doi.org/10.1016/j.micinf.2004.09.011.

Borges, C.L., Parente, J.A., Barbosa, M.S., Santa, J.M., Báo, S.N., de Sousa, M.V., de Almeida Soares, C.M., 2010. Detection of a homotetrameric structure and protein-protein interactions of *Paracoccidioides brasiliensis* formamidase lead to new functional insights. FEMS Yeast Res. 10, 104–113. https://doi.org/10.1111/j.1567-1364.2009.00594.x.

Brock, M., Buckel, W., 2004. On the mechanism of action of the antifungal agent propionate. Propionyl-CoA inhibits glucose metabolism in *Aspergillus nidulans*. Eur. J. Biochem. 271, 3227–3241. https://doi.org/10.1111/j.1432-1033.2004.04255.x.

Brock, M., Fischer, R., Linder, D., Buckel, W., 2000. Methylcitrate synthase from *Aspergillus nidulans*: implications for propionate as an antifungal agent. Mol. Microbiol. 35, 961–973. https://doi.org/10.1046/j.1365-2958.2000.01737.x.

Brown, G.D., Taylor, P.R., Reid, D.M., Willment, J.A., Williams, D.L., Martinez-Pomares, L., Wong, S.Y.C., Gordon, S., 2002. Dectin-1 is a major beta-glucan receptor on macrophages. J. Exp. Med. 196, 407–412. https://doi.org/10.1084/jem.20020470.

Butler, G., 2013. Hypoxia and gene expression in eukaryotic microbes. Annu. Rev. Microbiol. 67, 291–312. https://doi.org/10.1146/annurev-micro-092412-155658.

Camarasa, C., Faucet, V., Dequin, S., 2007. Role in anaerobiosis of the isoenzymes for *Saccharomyces cerevisiae* fumarate reductase encoded by OSM1 and FRDS1. Yeast 24, 391–401. https://doi.org/10.1002/yea.1467.

Cazzulo, J.J., 1992. Aerobic fermentation of glucose by trypanosomatids. FASEB J. 6, 3153–3161. https://doi.org/10.1096/fasebj.6.13.1397837.

Chae, H.Z., Rhee, S.G., 1994. A thiol-specific antioxidant and sequence homology to various proteins of unknown function. BioFactors (Oxford, England) 4, 177–180.

Chang, Y.C., Bien, C.M., Lee, H., Espenshade, P.J., Kwon-Chung, K.J., 2007. Sre1p, a regulator of oxygen sensing and sterol homeostasis, is required for virulence in *Cryptococcus neoformans*. Mol. Microbiol. 64, 614–629. https://doi.org/10.1111/j.1365-2958.2007.05676.x.

Chaves, A.F.A.A., Castilho, D.G., Navarro, M.V., Oliveira, A.K., Serrano, S.M.T.T., Tashima, A.K., Batista, W.L., 2017. Phosphosite-specific regulation of the oxidative-stress response of *Paracoccidioides brasiliensis*: a shotgun phosphoproteomic analysis. Microbes Infect. 19, 34–46. https://doi.org/10.1016/j.micinf.2016.08.004.

Chaves, E.G.A., Parente-Rocha, J.A., Baeza, L.C., Araújo, D.S., Borges, C.L., Oliveira, M. A.Pde, Soares, C.Mde A., 2019. Proteomic analysis of *Paracoccidioides brasiliensis* during infection of alveolar macrophages primed or not by interferon-gamma. Front. Microbiol. 10 https://doi.org/10.3389/fmicb.2019.00096.

Christie, D.A., Powell, J.W., Stables, J.N., Watt, R.A., 1987. A nuclear magnetic resonance study of the role of phosphoenol pyruvate carboxykinase (PEPCK) in the glucose metabolism of *Dipetalonema viteae*. Mol. Biochem. Parasitol. 24, 125–130. https://doi.org/10.1016/0166-6851(87)90098-3.

Chun, C.D., Liu, O.W., Madhani, H.D., 2007. A link between virulence and homeostatic responses to hypoxia during infection by the human fungal pathogen *Cryptococcus neoformans*. PLoS Pathog. 3 https://doi.org/10.1371/journal.ppat.0030022.

Claiborne, A., Yeh, J.I., Mallett, T.C., Luba, J., Crane, E.J., Charrier, V., Parsonage, D., 1999. Protein-sulfenic acids: diverse roles for an unlikely player in enzyme catalysis and redox regulation. Biochemistry 38, 15407–15416. https://doi.org/10.1021/bi992025k.

Coutinho, Z.F., Wanke, B., Travassos, C., Oliveira, R.M., Xavier, D.R., Coimbra, C.E.A., 2015. Hospital morbidity due to paracoccidioidomycosis in Brazil (1998-2006). Trop. Med. Int. Health 20, 673–680. https://doi.org/10.1111/tmi.12472.

Cymeryng, C., Cazzulo, J.J., Cannata, J.J.B., 1995. Phosphoenolpyruvate carboxykinase from *Trypanosoma cruzi*. Purification and physicochemical and kinetic properties. Mol. Biochem. Parasitol. 73, 91–101. https://doi.org/10.1016/0166-6851(95)00099-M.

de Curcio, J.S., Silva, M.G., Silva Bailão, M.G., Báo, S.N., Casaletti, L., Bailão, A.M., de Almeida Soares, C.M., 2017. Identification of membrane proteome of *Paracoccidioides lutzii*and its regulation by zinc. Future Sci. OA 3, FSO232. https://doi.org/10.4155/fsoa-2017-0044.

de Groot, M.J.L., Daran-Lapujade, P., van Breukelen, B., Knijnenburg, T.A., de Hulster, E. A.F., Reinders, M.J.T., Pronk, J.T., Heck, A.J.R., Slijper, M., 2007. Quantitative proteomics and transcriptomics of anaerobic and aerobic yeast cultures reveals post-transcriptional regulation of key cellular processes. Microbiology 153, 3864–3878. https://doi.org/10.1099/mic.0.2007/009969-0.

de Oliveira, A.R., Oliveira, L.N., Chaves, E.G.A., Weber, S.S., Bailão, A.M., Parente-Rocha, J.A., Baeza, L.C., de Almeida Soares, C.M., Borges, C.L., 2018. Characterization of extracellular proteins in members of the *Paracoccidioides* complex. Fungal Biol. 122, 738–751. https://doi.org/10.1016/j.funbio.2018.04.001.

Dhingra, S., Cramer, R.A., 2017. Regulation of sterol biosynthesis in the human fungal pathogen *Aspergillus fumigatus*: opportunities for therapeutic development. Front. Microbiol. 8 https://doi.org/10.3389/fmicb.2017.00092.

do Amaral, C.C., Fernandes, G.F., Rodrigues, A.M., Burger, E., de Camargo, Z.P., 2019. Proteomic analysis of *Paracoccidioides brasiliensis* complex isolates: correlation of the levels of differentially expressed proteins with in vivo virulence. PLoS One 14, e0218013. https://doi.org/10.1371/journal.pone.0218013.

Dubois, J.C., Pasula, R., Dade, J.E., Smulian, A.G., 2016. Yeast transcriptome and *in vivo* hypoxia detection reveals *Histoplasma capsulatum* response to low oxygen tension. Med Mycol. 40–58.

Eram, M.S., Ma, K., 2013. Decarboxylation of pyruvate to acetaldehyde for ethanol production by hyperthermophiles. Biomolecules 3, 578–596. https://doi.org/10.3390/biom3030578.

Erecińska, M., Silver, I.A., 2001. Tissue oxygen tension and brain sensitivity to hypoxia. Respir. Physiol. 128, 263–276. https://doi.org/10.1016/s0034-5687(01)00306-1.

Espenshade, P.J., 2006. SREBPs: sterol-regulated transcription factors. J. Cell. Sci. 119, 973–976. https://doi.org/10.1242/jcs02866.

Espenshade, P.J., Hughes, A.L., 2007. Regulation of sterol synthesis in eukaryotes. Annu. Rev. Genet. 41, 401–427. https://doi.org/10.1146/annurev.genet.41.110306.130315.

Felipe, M.S.S., Andrade, R.V., Arraes, F.B.M., Nicola, A.M., Maranhão, A.Q., Torres, F.A. G., Silva-Pereira, I., Poças-Fonseca, M.J., Campos, E.G., Moraes, L.M.P., Andrade, P. A., Tavares, A.H.F.P., Silva, S.S., Kyaw, C.M., Souza, D.P., Pereira, M., Jesuíno, R.S. A., Andrade, E.V., Parente, J.A., Oliveira, G.S., Barbosa, M.S., Martins, N.F., Fachin, A.L., Cardoso, R.S., Passos, G.A.S., Almeida, N.F., Walter, M.E.M.T., Soares, C.M.A., Carvalho, M.J.A., Brígido, M.M., Network, Pb Genome, 2005. Transcriptional profiles of the human pathogenic fungus *Paracoccidioides brasiliensis* in mycelium and yeast cells. J. Biol. Chem. 280, 24706–24714. https://doi.org/10.1074/jbc.M500625200.

Fraser, J.A., Davis, M.A., Hynes, M.J., 2001. The formamidase gene of *Aspergillus nidulans*: regulation by nitrogen metabolite repression and transcriptional interference by an overlapping upstream gene. Genetics 157, 119–131.

Gantner, B.N., Simmons, R.M., Canavera, S.J., Akira, S., Underhill, D.M., 2003. Collaborative induction of inflammatory responses by Dectin-1 and toll-like receptor 2. J. Exp. Med. 197, 1107–1117. https://doi.org/10.1084/jem.20021787.

Goldie, H., 1984. Regulation of transcription of the *Escherichia coli* phosphoenolpyruvate carboxykinase locus: studies with pck-lacZ operon fusions. J. Bacteriol. 159, 832–836. https://doi.org/10.1128/JB.159.3.832-836.1984.

Goldie, A.H., Sanwal, B.D., 1980. Genetic and physiological characterization of *Escherichia coli* mutants deficient in phosphoenolpyruvate carboxykinase activity. J. Bacteriol. 141, 1115–1121.

González Siso, M.I., Becerra, M., Lamas Maceiras, M., Vizoso Vázquez, A., Cerdán, M.E., 2012. The yeast hypoxic responses, resources for new biotechnological opportunities. Biotechnol. Lett. 34, 2161–2173. https://doi.org/10.1007/s10529-012-1039-8.

Grahl, N., Puttikamonkul, S., Macdonald, J.M., Gamcsik, M.P., Ngo, L.Y., Hohl, T.M., Cramer, R.A., 2011. In vivo hypoxia and a fungal alcohol dehydrogenase influence the pathogenesis of invasive pulmonary aspergillosis. PLoS Pathog. 7, e1002145 https://doi.org/10.1371/journal.ppat.1002145.

Grahl, N., Shepardson, K.M., Chung, D., Cramer, R.A., 2012. Hypoxia and fungal pathogenesis: to air or not to air? Eukaryot. Cell 11, 560–570. https://doi.org/10.1128/EC.00031-12.

Grosskaus, D.A., Bailão, A.M., Vieira Rezende, T.C., Borges, C.L., de Oliveira, M.A.P., Parente, J.A., de Almeida Soares, C.M., de Arruda Grosskaus, D., Bailão, A.M., Vieira Rezende, T.C., Borges, C.L., de Oliveira, M.A.P., Parente, J.A., de Almeida Soares, C. M., 2013. Response to oxidative stress in *Paracoccidioides* yeast cells as determined by proteomic analysis. Microbes Infect. 15, 347–364. https://doi.org/10.1016/j.micinf.2012.12.002.

He, G., Shankar, R.A., Chzhan, M., Samouilov, A., Kuppusamy, P., Zweier, J.L., 1999. Noninvasive measurement of anatomic structure and intraluminal oxygenation in the gastrointestinal tract of living mice with spatial and spectral EPR imaging. Proc. Natl. Acad. Sci. U. S. A. 96, 4586–4591.

Hillmann, F., Linde, J., Beckmann, N., Cyrulies, M., Strassburger, M., Heinekamp, T., Haas, H., Guthke, R., Kniemeyer, O., Brakhage, A.A., 2014. The novel globin protein fungoglobin is involved in low oxygen adaptation of *Aspergillus fumigatus*. Mol. Microbiol. 93, 539–553. https://doi.org/10.1111/mmi.12679.

Hillmann, F., Shekhova, E., Kniemeyer, O., 2015. Insights into the cellular responses to hypoxia in filamentous fungi. Curr. Genet. 61, 441–455. https://doi.org/10.1007/s00294-015-0487-9.

Hughes, A.L., Todd, B.L., Espenshade, P.J., 2005. SREBP pathway responds to sterols and functions as an oxygen sensor in fission yeast. Cell 120, 831–842. https://doi.org/10.1016/j.cell.2005.01.012.

Karhausen, J., Furuta, G.T., Tomaszewski, J.E., Johnson, R.S., Colgan, S.P., Haase, V.H., 2004. Epithelial hypoxia-inducible factor-1 is protective in murine experimental colitis. J. Clin. Invest. 114, 1098–1106. https://doi.org/10.1172/JCI21086.

Karst, F., Lacroute, F., 1977. Ertosterol biosynthesis in *Saccharomyces cerevisiae*: mutants deficient in the early steps of the pathway. Mol. Gen. Genet. 154, 269–277.

Ketelut-Carneiro, N., Silva, G.K., Rocha, F.A., Milanezi, C.M., Cavalcanti-Neto, F.F., Zamboni, D.S., Silva, J.S., 2015. IL-18 triggered by the Nlrp3 inflammasome induces host innate resistance in a pulmonary model of fungal infection. J. Immunol. 194, 4507–4517. https://doi.org/10.4049/jimmunol.1402321.

Knoops, B., Goemaere, J., Van der Eecken, V., Declercq, J.-P., 2011. Peroxiredoxin 5: structure, mechanism, and function of the mammalian atypical 2-Cys peroxiredoxin. Antioxid. Redox Signal. 15, 817–829. https://doi.org/10.1089/ars.2010.3584.

Koselny, K., Mutlu, N., Minard, A.Y., Kumar, A., Krysan, D.J., Wellington, M., 2018. A genome-wide screen of deletion mutants in the filamentous *Saccharomyces cerevisiae* background identifies ergosterol as a direct trigger of macrophage pyroptosis. mBio 9. https://doi.org/10.1128/mBio.01204-18.

Lee, H., Bien, C.M., Hughes, A.L., Espenshade, P.J., Kwon-Chung, K.J., Chang, Y.C., 2007. Cobalt chloride, a hypoxia-mimicking agent, targets sterol synthesis in the pathogenic fungus *Cryptococcus neoformans*. Mol. Microbiol. 65, 1018–1033. https://doi.org/10.1111/j.1365-2958.2007.05844.x.

Lima, Pde S., Casaletti, L., Bailão, A.M., Vasconcelos, A.T.Rde, Fernandes, Gda R., Soares, C.Mde A., 2014. Transcriptional and Proteomic Responses to Carbon Starvation in*Paracoccidioides*. PLoS Negl. Trop. Dis. 8 https://doi.org/10.1371/journal.pntd.0002855.

Lima, P.de S., Chung, D., Bailão, A.M., Cramer, R.A., Soares, C.Mde A., 2015. Characterization of the *Paracoccidioides*hypoxia response reveals new insights into pathogenesis mechanisms of this important human pathogenic fungus. PLoS Negl. Trop. Dis. 9, 1–25. https://doi.org/10.1371/journal.pntd.0004282.

Liu, X., Lieberman, J., 2017. A mechanistic understanding of pyroptosis: the fiery death triggered by invasive infection. Adv. Immunol. 135, 81–117. https://doi.org/10.1016/bs.ai.2017.02.002.

Marchitti, S.A., Brocker, C., Stagos, D., Vasiliou, V., 2008. Non-P450 aldehyde oxidizing enzymes: the aldehyde dehydrogenase superfamily. Expert Opin. Drug Metab. Toxicol. 4, 697–720. https://doi.org/10.1517/17425255.4.6.697.

Marcos, C.M., de Oliveira, H.C., da Silva, J., de, F., Assato, P.A., Fusco-Almeida, A.M., Mendes-Giannini, M.J.S., 2014. The multifaceted roles of metabolic enzymes in the *Paracoccidioides* species complex. Front. Microbiol. 5 https://doi.org/10.3389/fmicb.2014.00719.

Martinez, R., 2017. New trends in paracoccidioidomycosis epidemiology. J. Fungi (Basel) 3. https://doi.org/10.3390/jof3010001.

Masuo, S., Terabayashi, Y., Shimizu, M., Fujii, T., Kitazume, T., Takaya, N., 2010. Global gene expression analysis of *Aspergillus nidulans* reveals metabolic shift and transcription suppression under hypoxia. Mol. Genet. Genomics 284, 415–424. https://doi.org/10.1007/s00438-010-0576-x.

Matte, A., Tari, L.W., Goldie, H., Delbaere, L.T., 1997. Structure and mechanism of phosphoenolpyruvate carboxykinase. J. Biol. Chem. 272, 8105–8108. https://doi.org/10.1074/jbc.272.13.8105.

Mendes, R.P., Cavalcante, Rde S., Marques, S.A., Marques, M.E.A., Venturini, J., Sylvestre, T.F., Paniago, A.M.M., Pereira, A.C., da Silva, Jde F., Fabro, A.T., Bosco, Sde M.G., Bagagli, E., Hahn, R.C., Levorato, A.D., 2017. Paracoccidioidomycosis: current perspectives from Brazil. Open Microbiol. J. 11, 224–282. https://doi.org/10.2174/1874285801711010224.

Mendes-Giannini, M.J.S., Soares, C.P., da Silva, J.L.M., Andreotti, P.F., 2005. Interaction of pathogenic fungi with host cells: molecular and cellular approaches. FEMS Immunol. Med. Microbiol. 45, 383–394. https://doi.org/10.1016/j.femsim.2005.05.014.

Murad, A.M., Rech, E.L., 2012. NanoUPLC-MS^{E} proteomic data assessment of soybean seeds using the Uniprot database. BMC Biotechnol. 12, 82. https://doi.org/10.1186/1472-6750-12-82.

Nelson, D.L., Cox, M., 2014. Princípios de Bioquímica de Lehninger, 6th ed. Artmed, Porto Alegre.

Neto, B.Rda S., Carvalho, P.F.Z., Bailão, A.M., Martins, W.S., de Almeida Soares, C.M., Pereira, M., 2014. Transcriptional profile of*Paracoccidioides*spp. in response to itraconazole. BMC Genomics 15, 254. https://doi.org/10.1186/1471-2164-15-254.

Oliveira, L.N., Gonçales, R.A., Silva, M.G., Melo Lima, R.M., Tomazett, M.V., de Curcio, J. S., Paccez, J.D., Cruz-Leite, V.R.M., Rodrigues, F., Lima, Pde S., Pereira, M., Soares, C.Mde A., 2020. Characterization of a heme-protein responsive to hypoxia in *Paracoccidioides brasiliensis*. Fungal Genet. Biol. 144, 103446 https://doi.org/10.1016/j.fgb.2020.103446.

Parente, A.F.A., Bailão, A.M., Borges, C.L., Parente, J.A., Magalhães, A.D., Ricart, C.A.O., Soares, C.M.A., 2011. Proteomic analysis reveals that iron availability alters the metabolic status of the pathogenic fungus *Paracoccidioides brasiliensis*. PLoS One 6. https://doi.org/10.1371/journal.pone.0022810.

Parente, A.F.A., de Rezende, T.C.V., de Castro, K.P., Bailão, A.M., Parente, J.A., Borges, C.L., Silva, L.P., Soares, C.Mde A., 2013. A proteomic view of the response of *Paracoccidioides* yeast cells to zinc deprivation. Fungal Biol. 117, 399–410. https://doi.org/10.1016/j.funbio.2013.04.004.

Parente, A.F.A., Naves, P.E.C., Pigosso, L.L., Casaletti, L., McEwen, J.G., Parente-Rocha, J.A., Soares, C.M.A., 2015. The response of *Paracoccidioides*spp. to nitrosative stress. Microbes Infect. 17, 575–585. https://doi.org/10.1016/j.micinf.2015.03.012.

Parente-Rocha, J.A., Parente, A.F.A., Baeza, L.C., Bonfim, S.M.R.C., Hernandez, O., McEwen, J.G., Bailão, A.M., Taborda, C.P., Borges, C.L., Soares, C.Mde A., 2015. Macrophage interaction with *Paracoccidioides brasiliensis* yeast cells modulates fungal metabolism and generates a response to oxidative stress. PLoS One 10, e0137619. https://doi.org/10.1371/journal.pone.0137619.

Perez-Riverol, Y., Csordas, A., Bai, J., Bernal-Llinares, M., Hewapathirana, S., Kundu, D. J., Inuganti, A., Griss, J., Mayer, G., Eisenacher, M., Pérez, E., Uszkoreit, J., Pfeuffer, J., Sachsenberg, T., Yilmaz, S., Tiwary, S., Cox, J., Audain, E., Walzer, M., Jarnuczak, A.F., Ternent, T., Brazma, A., Vizcaíno, J.A., 2019. The PRIDE database and related tools and resources in 2019: improving support for quantification data. Nucleic Acids Res. 47, D442–D450. https://doi.org/10.1093/nar/gky1106.

Petito, G., de Curcio, J.S., Pereira, M., Bailão, A.M., Paccez, J.D., Tristão, G.B., de Morais, C.O.B., de Souza, M.V., de Castro Moreira Santos, A.J., Fontes, W., Ricart, C. A.O., de Almeida Soares, C.M., 2020. Metabolic adaptation of *Paracoccidioides brasiliensis* in response to in vitro copper deprivation. Front. Microbiol. 11 https://doi.org/10.3389/fmicb.2020.01834.

Pigosso, L.L., Parente, A.F.A., Coelho, A.S.G., Silva, L.P., Borges, C.L., Bailão, A.M., Soares, C.Mde A., 2013. Comparative proteomics in the genus *Paracoccidioides*. Fungal Genet. Biol. 60, 87–100. https://doi.org/10.1016/j.fgb.2013.07.008.

Pigosso, L.L., Baeza, L.C., Tomazett, M.V., Faleiro, M.B.R., de Moura, V.M.B.D., Bailão, A. M., Borges, C.L., Parente-Rocha, J.A., Fernandes, G.R., Gauthier, G.M., Soares, C. Mde A., 2017. *Paracoccidioides brasiliensis* presents metabolic reprogramming and secretes a serine proteinase during murine infection. Virulence 8, 1417–1434. https://doi.org/10.1080/21505594.2017.1355660.

Portis, I.G., de Sousa Lima, P., Paes, R.A., Oliveira, L.N., Pereira, C.A., Parente-Rocha, J. A., Pereira, M., Nosanchuk, J.D., de Almeida Soares, C.M., 2020. Copper overload in *Paracoccidioides lutzii* results in the accumulation of ergosterol and melanin. Microbiol. Res. 239, 126524 https://doi.org/10.1016/j.micres.2020.126524.

Prado, M., Silva, M.Bda, Laurenti, R., Travassos, L.R., Taborda, C.P., 2009. Mortality due to systemic mycoses as a primary cause of death or in association with AIDS in Brazil: a review from 1996 to 2006. Memórias do Instituto Oswaldo Cruz 104, 513–521. https://doi.org/10.1590/S0074-02762009000300019.

Queiroz, R.M.L., Charneau, S., Mandacaru, S.C., Schwämmle, V., Lima, B.D., Roepstorff, P., Ricart, C.A.O., 2014. Quantitative proteomic and phosphoproteomic analysis of *Trypanosoma cruzi* amastigogenesis. Mol. Cell. Proteom. 13, 3457–3472. https://doi.org/10.1074/mcp.M114.040329.

Queiroz-Telles, F., Fahal, A.H., Falci, D.R., Caceres, D.H., Chiller, T., Pasqualotto, A.C., 2017. Neglected endemic mycoses. Lancet Infect. Dis. 17, e367–e377. https://doi.org/10.1016/S1473-3099(17)30306-7.

Rappleye, C.A., Engle, J.T., Goldman, W.E., 2004. RNA interference in Histoplasma capsulatum demonstrates a role for α-(1,3)-glucan in virulence. Mol. Microbiol. 53, 153–165. https://doi.org/10.1111/j.1365-2958.2004.04131.x.

Rappleye, C.A., Eissenberg, L.G., Goldman, W.E., 2007. Histoplasma capsulatum alpha-(1,3)-glucan blocks innate immune recognition by the beta-glucan receptor. Proc. Natl. Acad. Sci. U. S. A. 104, 1366–1370. https://doi.org/10.1073/pnas.0609848104.

Rezende, T.C.V., Borges, C.L., Magalhães, A.D., de Sousa, M.V., Ricart, C.A.O., Bailão, A. M., Soares, C.M.A., 2011. A quantitative view of the morphological phases of *Paracoccidioides brasiliensis* using proteomics. J. Proteomics 75, 572–587. https://doi.org/10.1016/j.jprot.2011.08.020.

Rodrigues, M.L., 2018. The multifunctional fungal ergosterol. mBio 9. https://doi.org/10.1128/mBio.01755-18.

Rodrigues, M.L., Nosanchuk, J.D., 2020. Fungal diseases as neglected pathogens: a wake-up call to public health officials. PLoS Negl. Trop. Dis. 14, e0007964 https://doi.org/10.1371/journal.pntd.0007964.

Rodrigues, M.L., Nimrichter, L., Oliveira, D.L., Frases, S., Miranda, K., Zaragoza, O., Alvarez, M., Nakouzi, A., Feldmesser, M., Casadevall, A., 2007. Vesicular polysaccharide export in *Cryptococcus neoformans* is a eukaryotic solution to the problem of fungal trans-cell wall transport. Eukaryot. Cell 6, 48–59. https://doi.org/10.1128/EC.00318-06.

Rodrigues, L.Nda S., Brito, Wde A., Parente, A.F.A., Weber, S.S., Bailão, A.M., Casaletti, L., Borges, C.L., Soares, C.Mde A., 2016. Osmotic stress adaptation of *Paracoccidioides lutzii*, *Pb*01, monitored by proteomics. Fungal Genet. Biol. 95, 13–23. https://doi.org/10.1016/j.fgb.2016.08.001.

San-Blas, G., San-Blas, F., Serrano, L.E., 1977. Host-parasite relationships in the yeastlike form of *Paracoccidioides brasiliensis* strain IVIC Pb9. Infect. Immun. 15, 343–346. https://doi.org/10.1128/IAI.15.2.343-346.1977.

Santos, L.P.A., Assunção, L., do, P., Lima, P., de, S., Tristão, G.B., Brock, M., Borges, C.L., Silva-Bailão, M.G., Soares, C.Mde A., Bailão, A.M., 2020. Propionate metabolism in a human pathogenic fungus: proteomic and biochemical analyses. IMA Fungus 11, 9. https://doi.org/10.1186/s43008-020-00029-9.

Schousboe, A., Waagepetersen, H.S., 2007. GABA: homeostatic and pharmacological aspects. Prog. Brain Res. 160, 9–19. https://doi.org/10.1016/S0079-6123(06)60002-2.

Setiadi, E.R., Doedt, T., Cottier, F., Noffz, C., Ernst, J.F., 2006. Transcriptional response of *Candida albicans* to hypoxia: linkage of oxygen sensing and Efg1p-regulatory networks. J. Mol. Biol. 361, 399–411. https://doi.org/10.1016/j.jmb.2006.06.040.

Shepardson, K.M., Ngo, L.Y., Aimanianda, V., Latgé, J.-P., Barker, B.M., Blosser, S.J., Iwakura, Y., Hohl, T.M., Cramer, R.A., 2013. Hypoxia enhances innate immune activation to *Aspergillus fumigatus* through cell wall modulation. Microbes Infect. 15, 259–269. https://doi.org/10.1016/j.micinf.2012.11.010.

Shikanai-Yasuda, M.A., Mendes, R.P., Colombo, A.L., Queiroz-Telles, Fde, Kono, A.S.G., Paniago, A.M.M., Nathan, A., Valle, A.C.Fdo, Bagagli, E., Benard, G., Ferreira, M.S., Teixeira, Mde M., Silva-Vergara, M.L., Pereira, R.M., Cavalcante, Rde S., Hahn, R., Durlacher, R.R., Khoury, Z., Camargo, Z.Pde, Moretti, M.L., Martinez, R., Shikanai-Yasuda, M.A., Mendes, R.P., Colombo, A.L., Queiroz-Telles, Fde, Kono, A.S.G.,

Paniago, A.M.M., Nathan, A., Valle, A.C.Fdo, Bagagli, E., Benard, G., Ferreira, M.S., Teixeira, Mde M., Silva-Vergara, M.L., Pereira, R.M., Cavalcante, Rde S., Hahn, R., Durlacher, R.R., Khoury, Z., Camargo, Z.Pde, Moretti, M.L., Martinez, R., 2017. Brazilian guidelines for the clinical management of paracoccidioidomycosis. Rev. Soc. Bras. Med. Trop. 50, 715–740. https://doi.org/10.1590/0037-8682-0230-2017.

Shimizu, M., Fujii, T., Masuo, S., Fujita, K., Takaya, N., 2009. Proteomic analysis of *Aspergillus nidulans*cultured under hypoxic conditions. Proteomics 9, 7–19. https://doi.org/10.1002/pmic.200701163.

Siqueira, I.M., Fraga, C.L.F., Amaral, A.C., Souza, A.C.O., Jerônimo, M.S., Correa, J.R., Magalhães, K.G., Inácio, C.A., Ribeiro, A.M., Burguel, P.H., Felipe, M.S., Tavares, A. H., Bocca, A.L., 2016. Distinct patterns of yeast cell morphology and host responses induced by representative strains of *Paracoccidioides brasiliensis*(*Pb*18) and *Paracoccidioides lutzii* (*Pb*01). Med. Mycol. 54, 177–188. https://doi.org/10.1093/mmy/myv072.

Skouloubris, S., Labigne, A., De Reuse, H., 1997. Identification and characterization of an aliphatic amidase in *Helicobacter pylori*. Mol. Microbiol. 25, 989–998. https://doi.org/10.1111/j.1365-2958.1997.mmi536.x.

Sorais, F., Barreto, L., Leal, J.A., Bernabé, M., San-Blas, G., Niño-Vega, G.A., 2010. Cell wall glucan synthases and GTPases in *Paracoccidioides brasiliensis*. Med. Mycol. 48, 35–47. https://doi.org/10.3109/13693780802713356.

Synnott, J.M., Guida, A., Mulhern-Haughey, S., Higgins, D.G., Butler, G., 2010. Regulation of the hypoxic response in *Candida albicans*. Eukaryot. Cell 9, 1734–1746. https://doi.org/10.1128/EC.00159-10.

Tavares, A.H., Fernandes, L., Bocca, A.L., Silva-Pereira, I., Felipe, M.S., 2015. Transcriptomic reprogramming of genus *Paracoccidioides*in dimorphism and host niches. Fungal Genet. Biol. 81, 98–109. https://doi.org/10.1016/j.fgb.2014.01.008.

Taylor, R.C., Brown, A.K., Singh, A., Bhatt, A., Besra, G.S., 2010. Characterization of a -hydroxybutyryl-CoA dehydrogenase from *Mycobacterium tuberculosis*. Microbiology 156, 1975–1982. https://doi.org/10.1099/mic.0.038802-0.

Teixeira, M., de, M., Theodoro, R.C., Oliveira, F.F.Mde, Machado, G.C., Hahn, R.C., Bagagli, E., San-Blas, G., Soares Felipe, M.S., 2014. *Paracoccidioides lutzii* sp. nov.: biological and clinical implications. Med. Mycol. 52, 19–28. https://doi.org/10.3109/13693786.2013.794311.

Teutschbein, J., Albrecht, D., Pötsch, M., Guthke, R., Aimanianda, V., Clavaud, C., Latgé, J.-P., Brakhage, A.A., Kniemeyer, O., 2010. Proteome profiling and functional classification of intracellular proteins from conidia of the human-pathogenic mold *Aspergillus fumigatus*. J. Proteome Res. 9, 3427–3442. https://doi.org/10.1021/pr9010684.

Tielens, A.G., Van Hellemond, J.J., 1998. The electron transport chain in anaerobically functioning eukaryotes. Biochim. Biophys. Acta 1365, 71–78.

Todd, B.L., Stewart, E.V., Burg, J.S., Hughes, A.L., Espenshade, P.J., 2006. Sterol regulatory element binding protein is a principal regulator of anaerobic gene expression in fission yeast. Mol. Cell. Biol. 26, 2817–2831. https://doi.org/10.1128/MCB.26.7.2817-2831.2006.

Tsukihara, T., Aoyama, H., Yamashita, E., Tomizaki, T., Yamaguchi, H., Shinzawa-Itoh, K., Nakashima, R., Yaono, R., Yoshikawa, S., 1995. Structures of metal sites of oxidized bovine heart cytochrome c oxidase at 2.8 A. Science 269, 1069–1074.

Tupe, S.G., Kulkarni, R.R., Shirazi, F., Sant, D.G., Joshi, S.P., Deshpande, M.V., 2015. Possible mechanism of antifungal phenazine-1-carboxamide from *Pseudomonas* sp. against dimorphic fungi *Benjaminiella poitrasii* and human pathogen *Candida albicans*. J. Appl. Microbiol. 118, 39–48. https://doi.org/10.1111/jam.12675.

Turissini, D.A., Gomez, O.M., Teixeira, M.M., McEwen, J.G., Matute, D.R., 2017. Species boundaries in the human pathogen *Paracoccidioides*. Fungal Genet. Biol. 106, 9–25. https://doi.org/10.1016/j.fgb.2017.05.007.

Uwamahoro, N., Verma-Gaur, J., Shen, H.-H., Qu, Y., Lewis, R., Lu, J., Bambery, K., Masters, S.L., Vince, J.E., Naderer, T., Traven, A., 2014. The pathogen *Candida albicans* hijacks pyroptosis for escape from macrophages. mBio 5, e00003–00014. https://doi.org/10.1128/mBio.00003-14.

Verleur, N., Elgersma, Y., Van Roermund, C.W., Tabak, H.F., Wanders, R.J., 1997. Cytosolic aspartate aminotransferase encoded by the AAT2 gene is targeted to the peroxisomes in oleate-grown *Saccharomyces cerevisiae*. Eur. J. Biochem. 247, 972–980.

Villén, J., Gygi, S.P., 2008. The SCX/IMAC enrichment approach for global phosphorylation analysis by mass spectrometry. Nat. Protoc. 3, 1630–1638. https://doi.org/10.1038/nprot.2008.150.

Vödisch, M., Scherlach, K., Winkler, R., Hertweck, C., Braun, H.-P.P., Roth, M., Haas, H., Werner, E.R., Brakhage, A.A., Kniemeyer, O., Vödisch, M., Scherlach, K., Winkler, R., Hertweck, C., Braun, H.-P.P., Roth, M., Haas, H., Werner, E.R., Brakhage, A.A., Kniemeyer, O., 2011. Analysis of the *Aspergillus fumigatus*proteome reveals metabolic changes and the activation of the pseurotin A biosynthesis gene cluster in response to hypoxia. J. Proteome Res. 10, 2508–2524. https://doi.org/10.1021/pr1012812.

Weber, S.S., Parente, A.F.A., Borges, C.L., Parente, J.A., Bailão, A.M., de Almeida Soares, C.M., 2012. Analysis of the secretomes of *Paracoccidioides* mycelia and yeast cells. PLoS One 7, e52470. https://doi.org/10.1371/journal.pone.0052470.

Wellington, M., Koselny, K., Sutterwala, F.S., Krysan, D.J., 2014. *Candida albicans* triggers NLRP3-mediated pyroptosis in macrophages. Eukaryot. Cell 13, 329–340. https://doi.org/10.1128/EC.00336-13.

Willger, S.D., Puttikamonkul, S., Kim, K.-H., Burritt, J.B., Grahl, N., Metzler, L.J., Barbuch, R., Bard, M., Lawrence, C.B., Cramer, R.A., 2008. A sterol-regulatory element binding protein is required for cell polarity, hypoxia adaptation, azole drug resistance, and virulence in *Aspergillus fumigatus*. PLoS Pathog. 4, e1000200 https://doi.org/10.1371/journal.ppat.1000200.

Yadav, A.K., Desai, P.R., Rai, M.N., Kaur, R., Ganesan, K., Bachhawat, A.K., 2011. Glutathione biosynthesis in the yeast pathogens *Candida glabrata* and *Candida albicans*: essential in *C. glabrata*, and essential for virulence in *C. albicans*. Microbiology (Reading) 157, 484–495. https://doi.org/10.1099/mic.0.045054-0.

Yao, L., Yang, Y., He, G., Ou, C., Wang, L., Liu, K., 2018. Global proteomics deciphered novel-function of osthole against pulmonary arterial hypertension. Sci. Rep. 8, 5556. https://doi.org/10.1038/s41598-018-23775-8.

Zhang, S., Zeng, X., Ren, M., Mao, X., Qiao, S., 2017. Novel metabolic and physiological functions of branched chain amino acids: a review. J. Anim. Sci. Biotechnol. 8 https://doi.org/10.1186/s40104-016-0139-z.